ULTRA HIGH FREQUENCY OSCILLATORS

Thesis by

Andrew V. Haeff.

In Partial Fulfillment of the Requirements for the

Degree of

Doctor of Philosophy

California Institute of Technology

Pasadena, California.

1932.

Contents.

1. SUMMARY.

The performance of three electrode tubes operating on the Barkhausen principle has been studied. Several tubes of different design have been constructed and tested. One particular design in which two extra leads were brought out from the grid and the plate, proved to be especially advantageous, because its minimum grid current was small, and the wavelength could be varied continuously throughout the region in which the tube produced oscillations. Normal waves and waves of the higher orders could be produced.

The effect of changing the position of electrodes with respect to the standing voltage wave was studied. It was found that tubes oscillate more easily if the electrodes are placed in the loop of the voltage wave. This study was made possible by the design of a special tube and the use of a special circuit.

The dependence of the minimum grid current upon the wavelength has been studied and it was found, that the theoretical relation $I_g = \frac{k}{\lambda^3}$ is only approximate: the coefficient "k" increases as the wavelength decreases.

The variation of the energy output with the emission current was studied and it was found, that the maximum energy output is obtained when the emission current reaches its static saturation value. Tests have shown that tubes with water cooled grids have characteristics similar to those of tubes having grids cooled by radiation.

2. INTRODUCTION.

Since the discovery by Barkhausen and Kurz in 1920 (Ref.1) of oscillations produced by a three electrode tube in which the grid has high positive potential, a considerable amount of work on the Barkhausen effect has been done by investigators in Germany, Russia, France and in this country. A very complete outline of the work done up to 1930 was published by H.E.Hollmann (Ref.2). This article contains also a very complete list of references.

To make further discussion clearer, the essential features of the Barkhausen oscillator will be considered here.

The fundamental circuit is represented in Fig.1. The grid is connected to the positive terminal of a D.C. generator or battery.

$$F i g. 1.$$

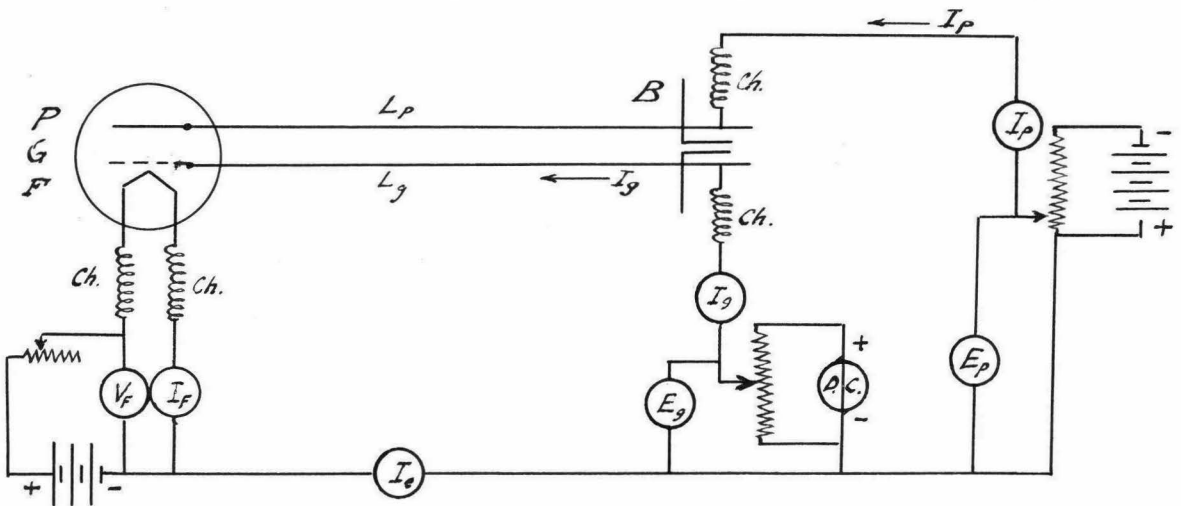The plate is held at zero (negative end of the filament) or negative potential. The oscillating circuit, usually consisting of two parallel wires, is connected to the grid and to the plate. The circuit is terminated by a condenser "B", which for the high frequency used represents practically a short circuit. High frequency chokes are placed in each lead, connecting the tube with the voltage supply.

Barkhausen found that the frequency of oscillations corresponds approximately to the frequency of electronic oscillations around the grid (Ref.1). This rule was later extended and modified (Ref.3,4) and can be stated as follows: The maximum energy output is obtained when the natural frequency of the oscillating circuit corresponds to the electronic frequency or its multiple. When the frequency is equal to the electronic frequency, the waves are called normal waves; when the frequency is some multiple of the electronic frequency, the waves are called high order waves (1st order, 2nd order, etc.).

The experiments of Kroebel (Ref.5) demonstrated that a considerable increase in the output was produced if the plate was made negative. Maximum energy was obtained when the plate current was reduced to zero.

Gill and Morell (Ref.6) were the first to observe the dependence of frequency upon the tuning of the external circuit. The so called "pure" Barkhausen oscillations, the frequency of which does not depend upon the tuning of the circuit, were later found to be produced only in exceptional cases. It is thought that "pure" B-K oscillations occur only if there is a sharply tuned circuit inside the tube, which is formed by the electrodes and the leads inside the tube. During the present investigation in no case "pure" B-K oscillations were observed.

The effect of symmetry in the arrangement of electrodes was studied by A.Wainberg (Ref.7), who has shown that with tubes having the filament or the grid displaced from the position concentric with the plate, no waves of higher orders could be obtained, and that in general, the dissymmetry reduced the output considerably both for normal and for high order waves.

The experimental study of Barkhausen oscillators was undertaken with the purpose of finding means of increasing the energy output in the shorter wave region. Early in the course of investigation it was observed that the capacitance between the electrodes and the wires forming the oscillating circuit had a considerable influence upon the operation of the tube. The distribution of standing waves along the oscillating circuit was then studied and it was found that the smaller the ratio of the capacitance between the electrodes to the capacitance per unit length of the oscillating circuit, the easier it is to produce oscillations. To be able to displace the electrodes with respect to the standing wave without detuning the circuit, a special tube was constructed. The results obtained with this tube will be described in the next paragraph.

Since the principle of operation of the Barkhausen oscillator differs radically from that of ordinary oscillators, special tubes were constructed. Part of the work has been done with tubes connected permanently to the evacuating system, consisting of a fore pump and a two stage mercury diffusion pump. The pressure was measured by means of a MacLeod gauge. The pressure of 10^{-4} to 10^{-5} mm.Hg. was usually maintained, between which limits the operation of the tube was not affected by changes in pressure (Ref.8). The tubes were made so that they could be easily opened for replacing the filament or for changing and adjusting the electrodes. Several tubes were made which after a thorough baking and heating of electrodes were completely sealed off the pump. In these tubes an extremely hard vacuum was obtained, the positive ion current at maximum loading (about 100 ma, 800 volts,) being only a few microamperes.

Only cylindrical electrodes were used, the filament and the grid being placed concentrically with the plate. Pure tungsten filaments were used. Grids were made of tungsten wire wound in the form of a spiral. Tungsten was used for grids, because the heat produced by the electronic bombardment is sufficient to melt metals with lower melting point (grids made of nickel melted readily even at low loading).

A 500-volt D.C. generator supplied the positive voltage to the grid. The voltage was varied by means of a potentiometer. A 45-volt "B" battery was used for negative bias on the plate. A 6-volt storage battery was used for heating the filament.

The oscillating circuit usually consisted of a Lecher wire system on which standing waves were formed. The reflecting condenser bridges were so designed that their natural frequency was considerably above the frequency of the circuit (Ref.9).

The methods used for measuring the wavelength and the amplitude of oscillations will be described in a later paragraph.

3. Effect of the change of the position of electrodes with

respect to the voltage wave.

(a). Description of apparatus.

Fig.2 and Fig.3 respectively show the general view of the apparatus and the construction of the tube. Fig.4 represents a schematic diagram of the circuit.

As can be seen from Figs. 3 and 4, connections to the plate and the grid are brought out at both ends of the tube, and are joined directly to the two oscillating circuits L_1 and L_2. The filament leads are bent at right angle to the oscillating circuit
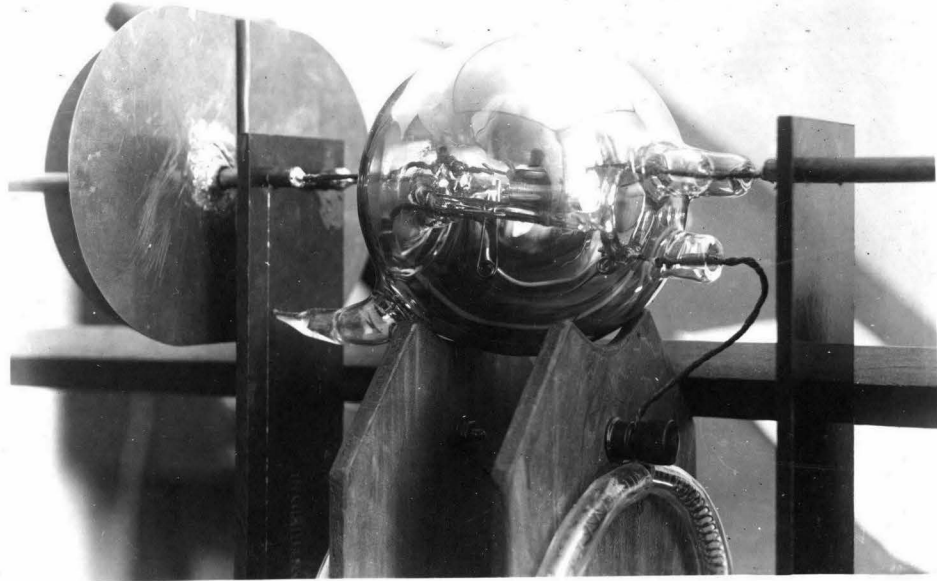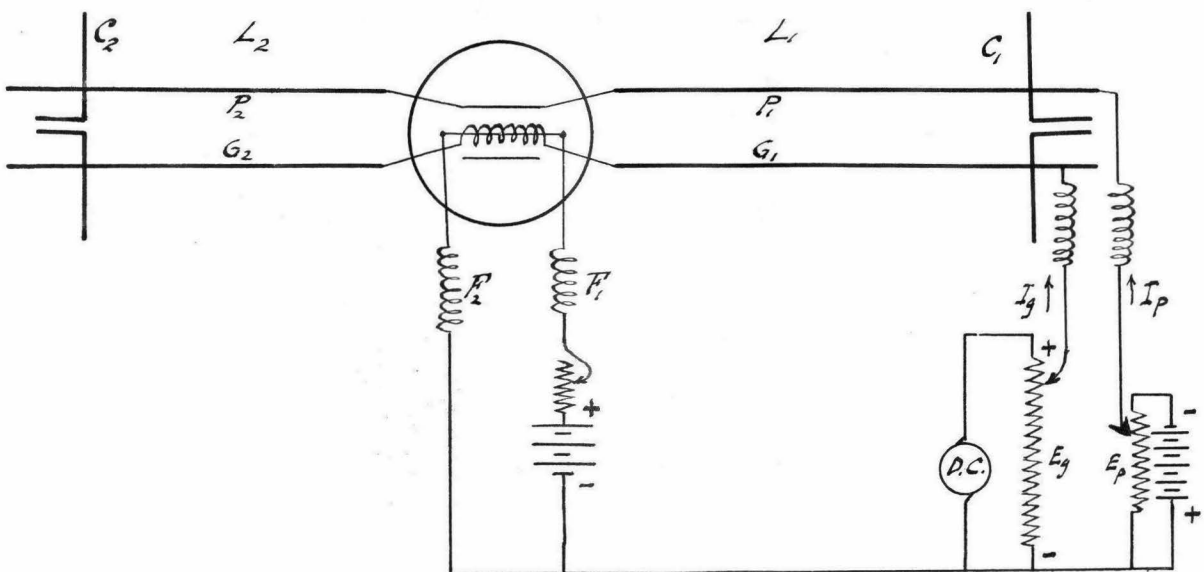
Fig.2.

Fig.3.

Fig.4.

and are connected directly to the chokes placed close to the tube. The Lecher system formed by the two circuits L_1 and L_2, is short circuited at the two ends by means of two condenser bridges C_1 and C_2. The grid and plate supply voltages (D.C.) are delivered to the circuit through R.F. chokes and the connections are made at the ends of the Lecher wires L_1 beyond the bridge C_1, where no standing waves are present.

b). Dependence of the amplitude of oscillations upon the position
of electrodes with respect to the standing wave.

The following effect has been observed. With the voltage and the grid current constant and the bridges C_1 and C_2 moved in the same direction along the wires so that their separation remained constant and the natural frequency of the circuit unchanged, the plate current was found to depend upon the position of the bridges. The constancy of frequency was checked by means of an auxiliary Lecher wire system used for measuring the wavelength (see p.43).

The results are shown on p.10. On the diagram the plate current I_p is plotted vertically, and the abscissa represents the position of the middle of the oscillating circuit. The center line of electrodes is marked by a dotted line 63 cm. from an arbitrary zero.

A marked decrease of the plate current occurs when the center line of the circuit is displaced from the center line of the electrodes. In other words, the plate current decreases when the A.C. voltage across the electrodes is less than the maximum A.C. voltage in the oscillating circuit.This result has been expected since the oscillations

Diagram 1.

Plate current (I) as a function
of the position of electrodes
with respect to the center of
the oscillating circuit.
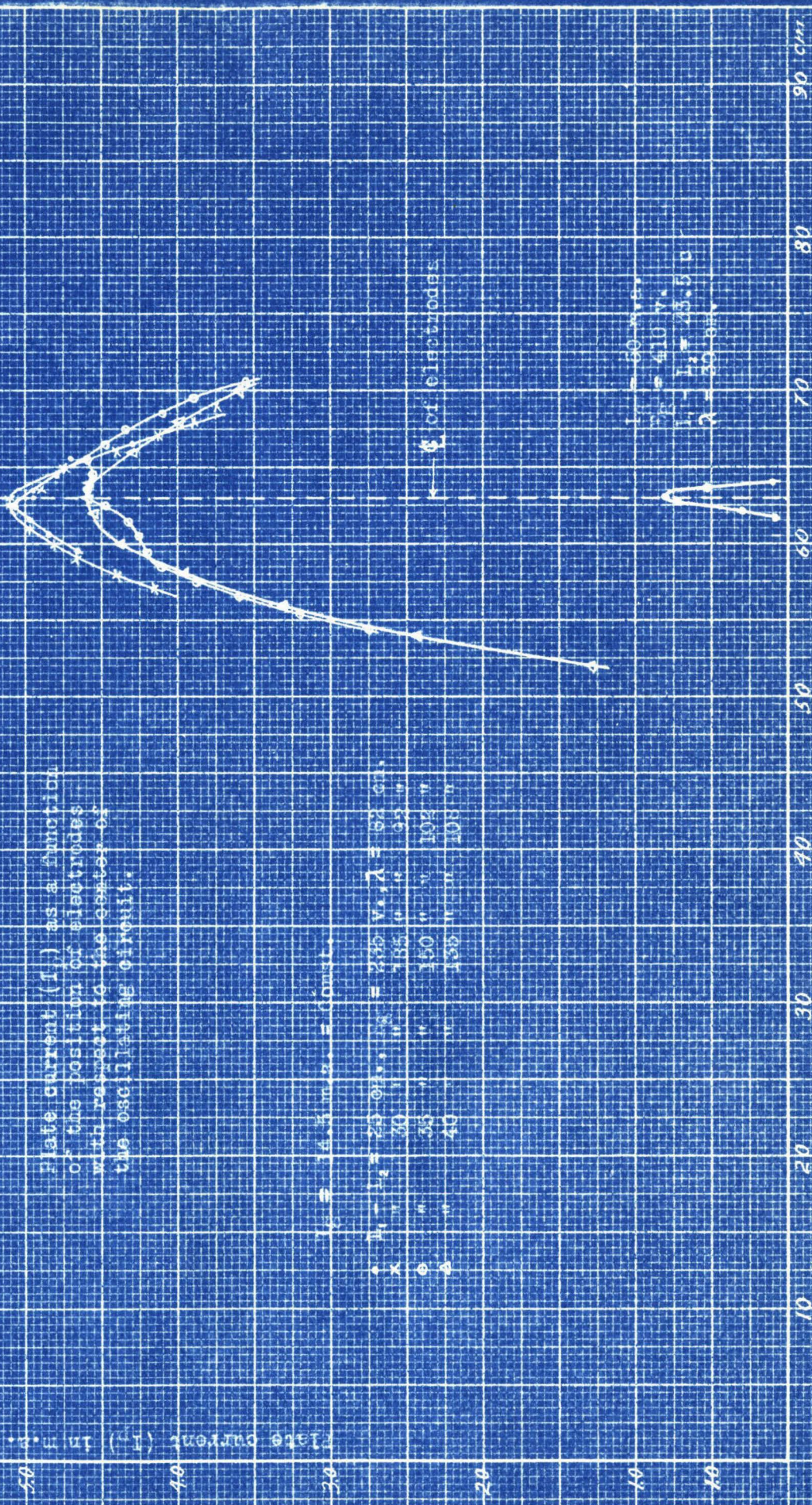
Center line of the oscillating circuit ... the auxiliary ...

Distance of center line of the oscillating circuit ... the auxiliary ...

Plate current (I) in m.a.

of the electronic space charge which cause the tube to oscillate, are produced by the A.C. voltages between the grid and plate. Thus, the conditions for oscillations are most favourable when the electrodes are placed in the loop of the voltage wave.

The same effect was observed for waves of different orders and for different wavelengths. For shorter waves, as for example for 30cm., the sharpness of the peak is very marked, and shows not only the importance of proper tuning of the circuit but also the necessity of placing the electrodes in the loop of the voltage wave. The method of doing this, as described above, using a special tube, is simple and effective, and of particular importance for short wavelengths.

The curves on p.12 show the change of the plate current as a function of the displacement of electrodes with respect to the position of the loop of the voltage wave expressed in percent of wavelength. It should be noted, however, that the shape of these curves depends upon the ratio of the grid current at which the tube is operated to its minimum value at which the oscillations begin.

Diagram 2.

Change of plate current
with the displacement
of electrodes

Grid current const.
Grid voltage const.
Circuit frequency const.

$\left(\dfrac{I_P}{I_{Pmax}}\right)$ %

$I_P = I_{Pmax}\left[1 - K\left(\dfrac{\Delta\ell}{\lambda}\right)^2\right]$

$K \approx 68$

$\dfrac{\Delta\ell}{\lambda}$ %
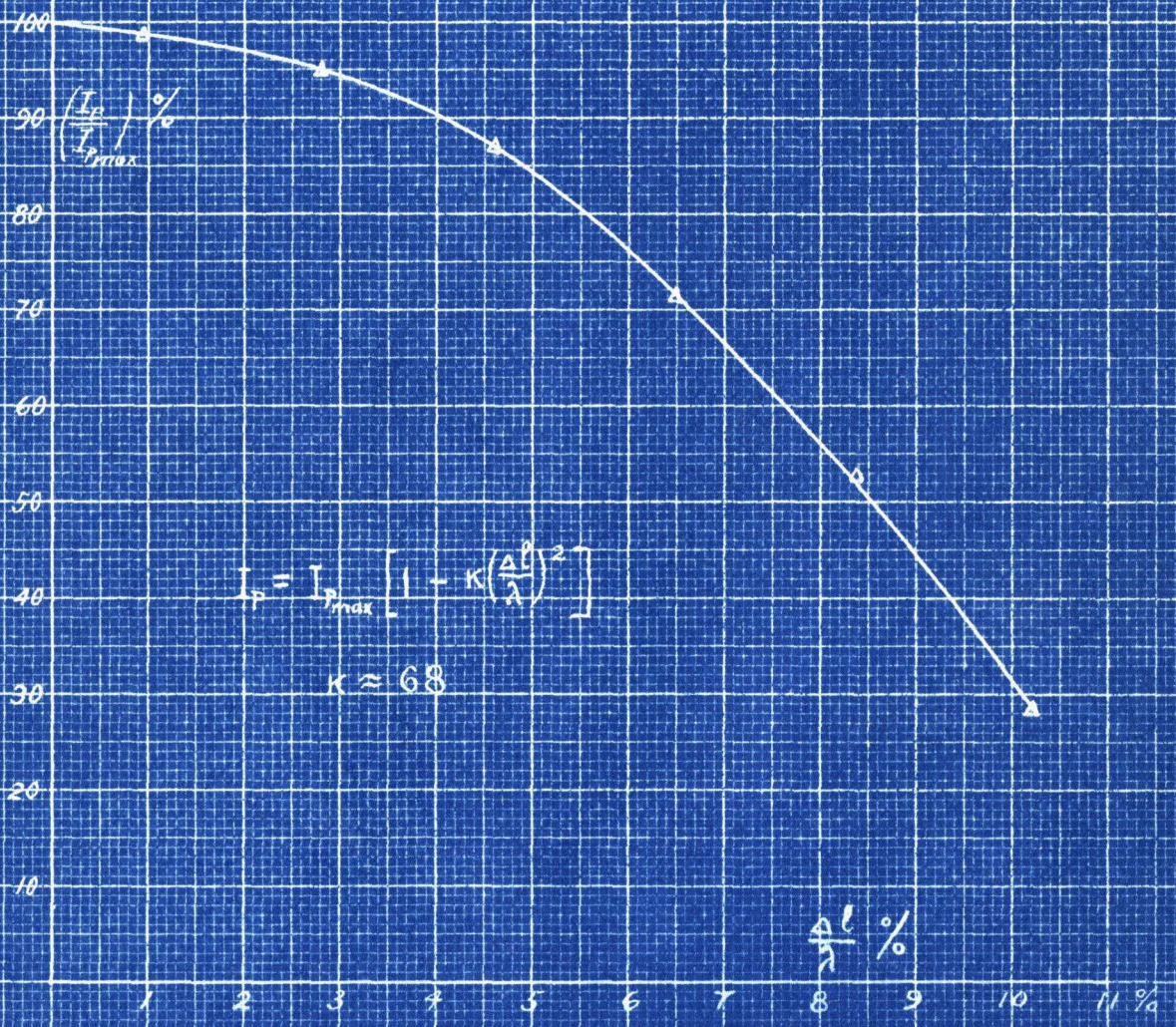
(c). Dependence of the required minimum grid current upon

the position of electrodes.

The importance of having electrodes in the loop of the voltage wave can be demonstrated in a striking manner by observing the minimum emission current at which the tube will oscillate. With constant grid voltage and frequency, this minimum grid current was observed for different positions of the bridges C_1 and C_2, the distance between them being kept constant. The results are shown on p.14. The minimum grid current occurs when the electrodes are in the center of the oscillating circuit, that is, in the loop of the voltage wave. The rapid increase of the required minimum grid current with the displacement of the electrodes from this center shows the importance of the proper tuning of the circuit, especially in the region of short waves.

The change of the grid current with the electrode displacement can be approximately expressed by the formula:

$$I_{g_\lambda} = I_{g_{min}}\left[1 + c_\lambda\left(\frac{\Delta\ell}{\lambda}\right)^2\right]$$

where

I_{g_λ} = the required minimum grid current for wavelength λ,

$I_g min.$ = minimum grid current for $\Delta\ell = 0$.

$\Delta\ell$ = the distance between the loop of the voltage wave and the
  center of electrodes,

λ = the wavelength, and

c_λ = coefficient depending upon λ. The approximate value of this coefficient is $c_\lambda = 1000$, so that for a displacement of $\frac{\Delta\ell}{\lambda} = 3\%$, the minimum grid current is twice its value for the central position of the electrodes.

Diagram 3.

Change of grid current
with the displacement
of electrodes.
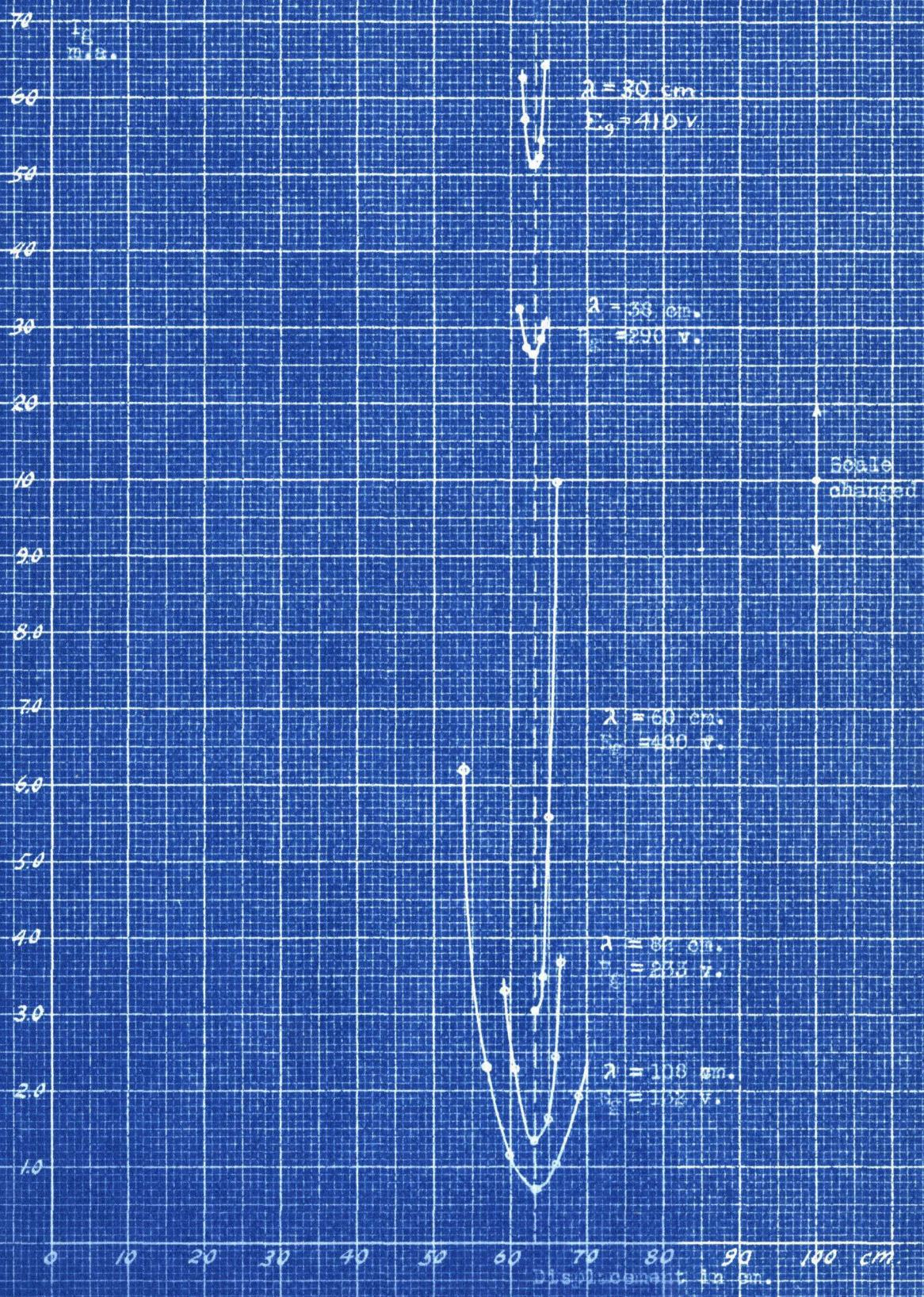
Diagram 4.

Min. grid current as a
function of displacement.
of electrodes.

% $\frac{I_g}{I_{g_{min}}}$ in %

$$I_g = I_{g_{min}} \left[1 + C_\lambda \left(\frac{\pi L}{\lambda} \right)^2 \right]$$

$$C_\lambda = 1000$$

$\cdot \; \lambda = 10 \; R$

$\times \; \lambda = 8 \; R$

$\ominus \; \lambda = 6 \; R$

Displacement $\frac{\pi L}{\lambda}$ in %
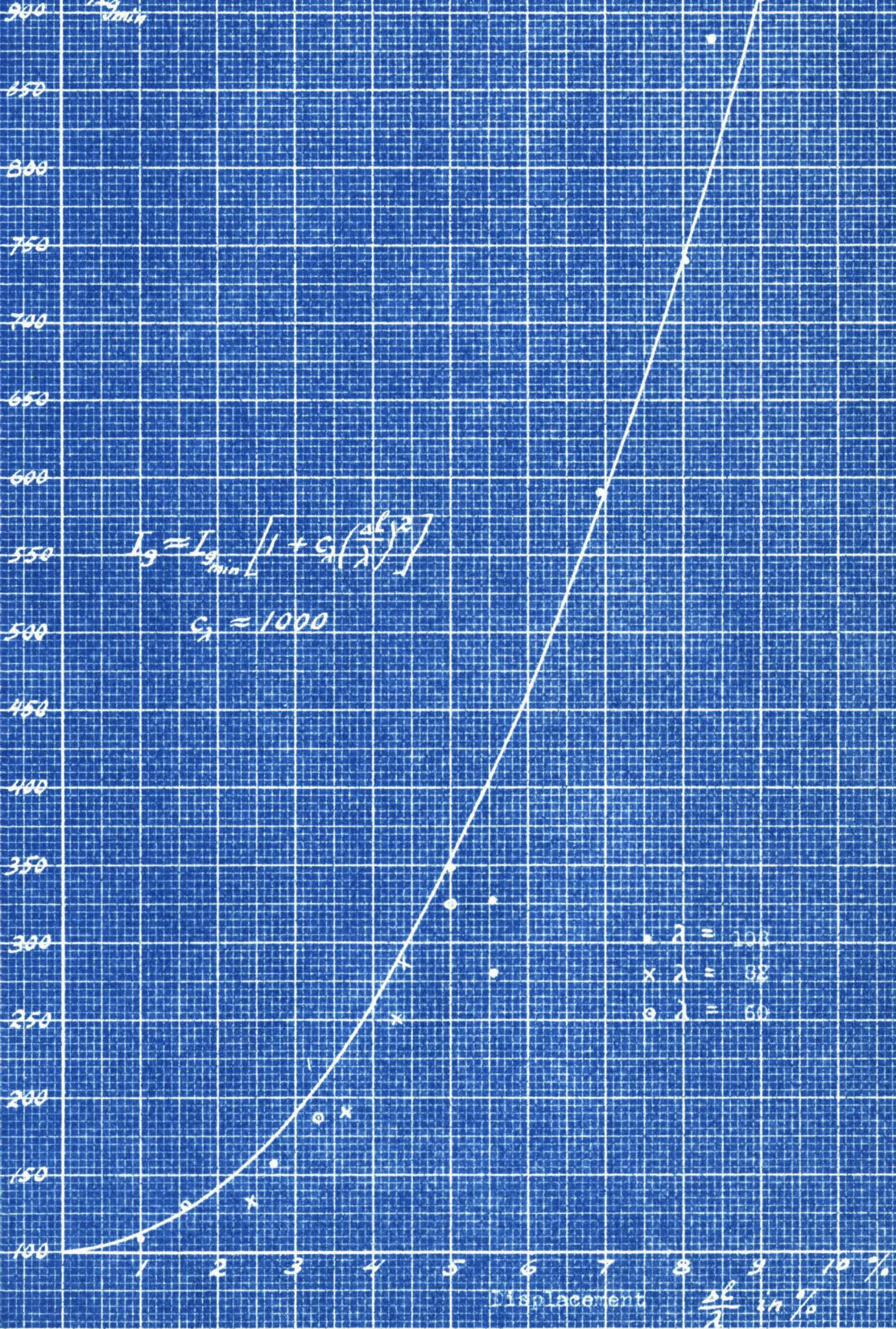
(d). Dependence of the minimum grid current upon the wavelength.

From the diagram on p.14 it can be seen that the minimum grid current (points marked "a") increases with decreasing wavelength. Minimum grid current as a function of wavelength is plotted on diagram 5, p.17.

In the middle region the curve can be approximately expressed by the followin equation:

$$I_{g_{min}} = \frac{Const}{\lambda^3}$$

This form of the function agrees with the one deduced from the theoretical considerations (Ref.10 and 11). The experimental curve, however, deviates from the theoretical curve especially in the region of short wavelengths, where the increase of the grid current is more rapid. In that region the importance of having the electrodes in the loop of the voltage wave is obvious, since for short wavelengths the minimum grid currents are high and any means for reducing the grid current are very desirable.

(e). Effect of the dissymmetry of the grid and plate circuits.

Due to a very rapid increase of emission current for shorter waves, it has not been possible to obtain waves below $\lambda = 25$ cm. with the tube used in the experiments described above. This may be due to the dissymmetry in the arrangement of electrodes, as at high emission the filament was slightly sagging. However, another peculiarity was also noticed, namely, the distribution of standing waves along the circuit was not symmetrical. The position of nodes on the plate wire "P" did not exactly coincide with the nodes on the grid wire "G", nodes on "G" being farther

Diagram 5.

Change of max. grid current
with wavelength.
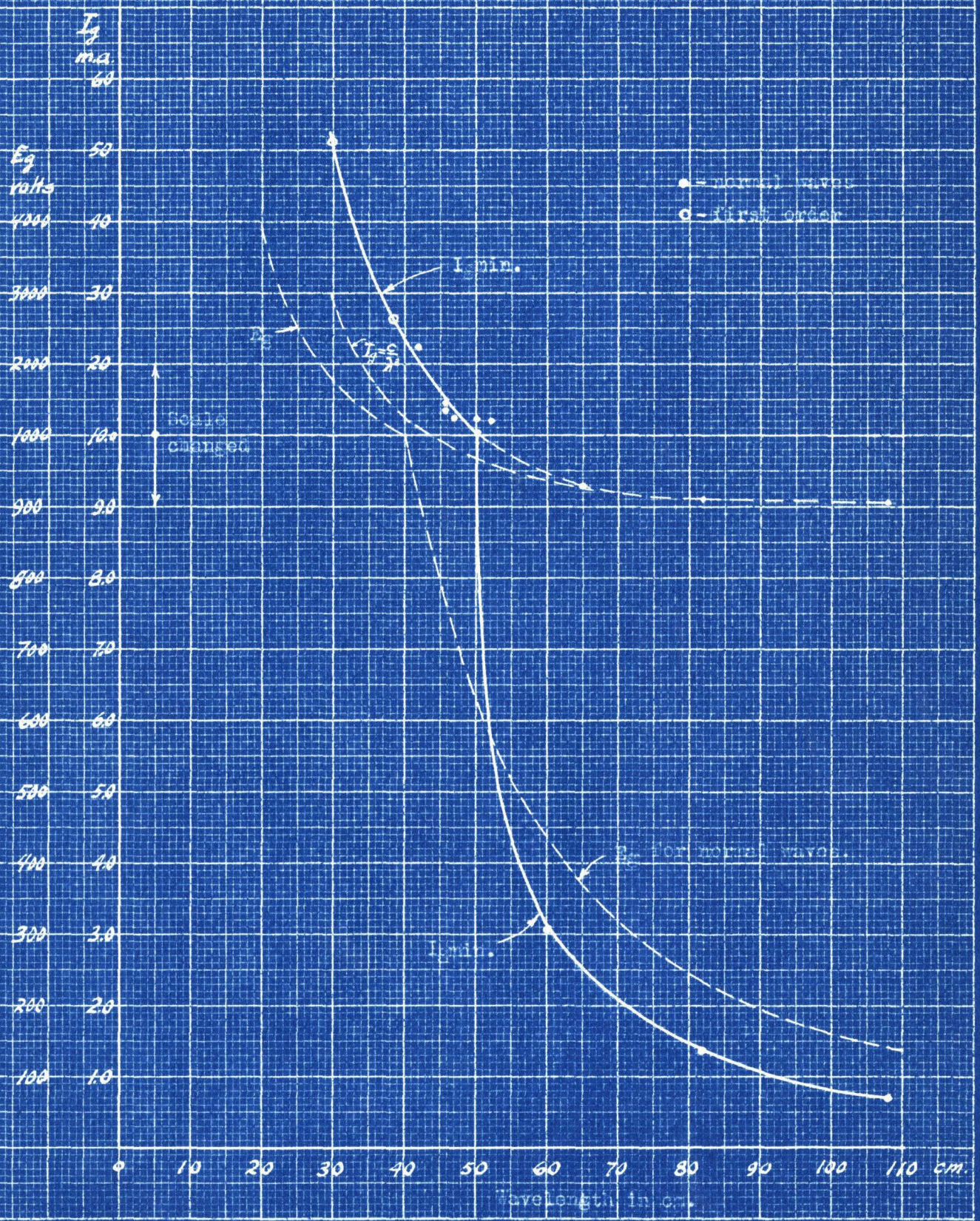
away from the tube, than the nodes on the "P" wire. Since the
"G" and "P" circuits are identical except for the electrodes,
this effect must be caused by the grid, having an effective length
which is evidently several times its actual length. By taking
into consideration the grid to plate capacitance and the inductance
of the grid spiral the distance between the bridges was calculated
for different wavelengths and the results were found in agreement
with the experimental values. However, the effective length of the
grid circuit was greater than the length of the plate circuit, when
the tuning bridges of the shape shown in Fig.4 were used. Hence, if
the grid circuit is tuned sharply to the most probable electronic
frequency or multiple thereof, the plate circuit is not so tuned,
and vice-versa. The fact that one of the circuits is not tuned is very
undesirable since this condition requires more energy expended in
the circuit to produce a given voltage between the grid and plate,
than is the case when the circuits are tuned simultaneously. This
effect is much more pronounced for shorter wavelengths, and may
wholly explain the rapid increase of the grid current with
increasing frequency.

To avoid this difficulty, the following remedies can be used:
(a) Separate tuning of the grid and of the plate circuits, (b) Change
in the construction of the grid by placing a supporting bar along
the grid and welding it to the grid, thus effectively short-circuiting
the grid, so its effective length would be equal to that of the plate.

The first method has been used by others for standard tubes with
apparently good results (Ref.3), although the importance of the

separate tuning has not been explained. For the special tube,
described above, which has two circuits on either side for the
purpose of placing the electrodes in the loop of the voltage wave,
the first method of obtaining symmetrical "P" and "G" circuits is
rather inconvenient. The displacement of the bridge C_{p1} with respect
to C_{g1} (see Fig.4), would affect the distribution of waves on "G",
which is undesirable. Another disadvantage is that the distribution
would still be unsymmetrical even if both P and G circuits were
tuned. Another modification of method (a) would be to make the "P"
and The "G" circuits intersect at right angles to each other (see F.5),
but this would considerably increase the radiation resistance of
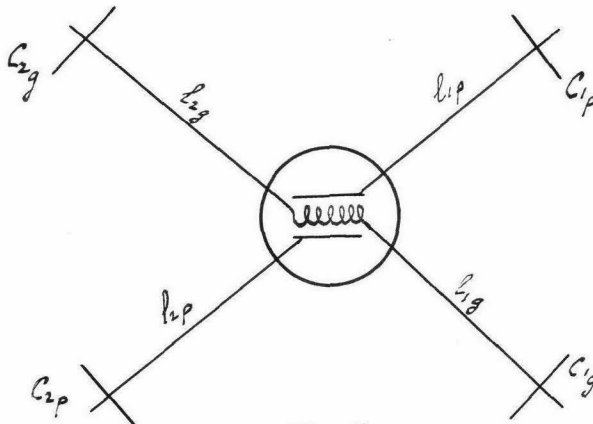the circuit.

Fig.5.

The second method, (b), will make it possible to obtain a
symmetrical distribution of waves throughout the length of the
circuit with the use of simple condenser bridges. At the present
moment a special tube is being built with particular attention being
given to the symmetry of the electrodes inside the tube, and of
the grid and plate circuits.

4. Analysis of the experimental results.

The following analysis is an attempt to explain the very rapid increase of the grid current with shortening of the wavelength. The experimental results presented, indicate that the minimum grid current depends upon the wavelength in the following manner:

$$I_{gmin} = \frac{k_1}{\lambda^2} + \frac{k_2}{\lambda^3} + \frac{k_3}{\lambda^4}$$

where k_1, k_2 and k_3 are constants of the tube. This form of the equation has been obtained from the analysis of the curve $I_g$min. shown on Dia.6. The theoretical value of $I_g$min., derived on the assumption of the same effective A.C. voltage throughout the length of the grid, (Ref.10), differs from the above in that $k_1 = k_3 = 0$. Hence it is desirable to analyze the conditions actually existing inside the tube, and to axplain why the theoretical assumption is not valid.

Another object of this analysis is to show that the observed rapid increase of $I_g$min. with the displacement of electrodes from the central position with respect to the voltage wave, is actually caused by a decrease in the effective A.C. voltage across the electrodes and is not due to the detuning of the oscillating circuit.

(a). Distribution of standing waves along the wires.

The distribution of waves along the wires forming the oscillating circuit is represented graphically on p.21. This distribution was found by determining the positions of voltage nodes and by wavelength measurements. Only the voltage wave is shown. The standing

Diagram 6.

Distribution of voltage waves
along the earth wire.

λ=30 cm.

λ=38 cm.

λ=48 cm.

λ=60

λ=82

λ=92

λ=142

λ=109

Position of

Distance in metres from middle of antenna

(21)
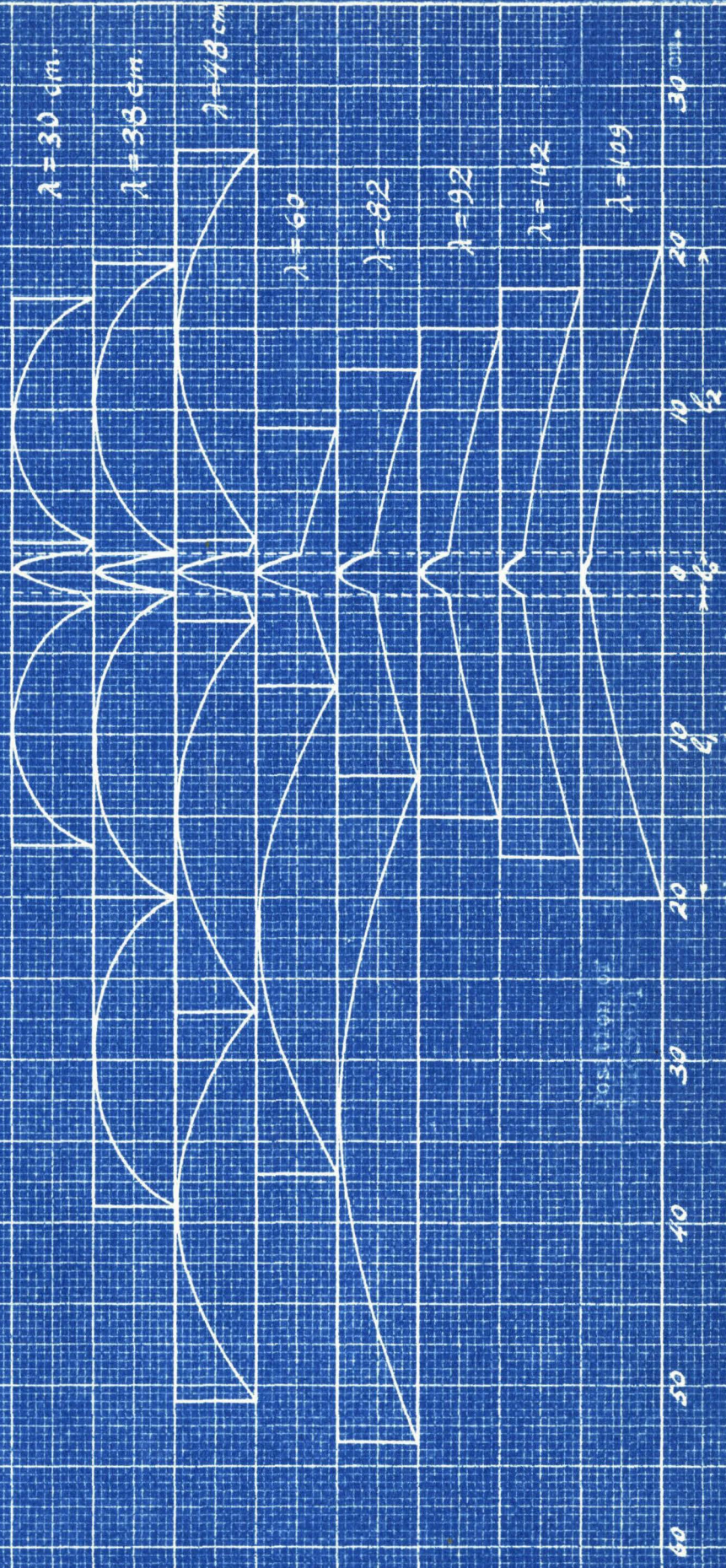
current wave would be displaced a quarter wavelength from the
position of the voltage wave, because the damping is very small.
Diagram 6 shows the distribution along the grid wire only. The
nodes on the plate wire, however, practically coincided with
the nodes on the grid wire.

(b). Effect of the grid to plate capacitance on the natural
frequency of the oscillating circuit.

The oscillating circuit consisting of the Lecher system, short-
circuited at the two ends and with the tube placed in the system,
can be shematically represented as is shown in Fig.6.
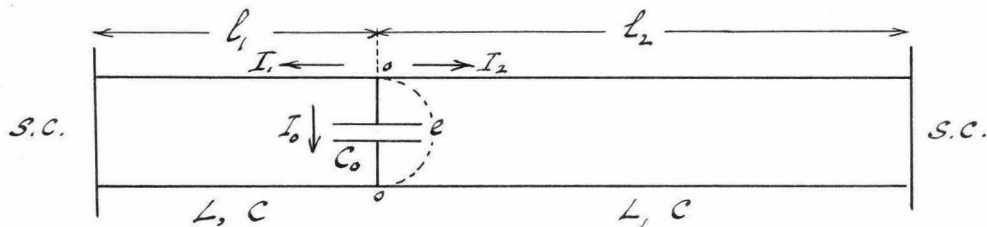
Fig.6.

C_0 represents the total grid to plate capacitance, L and C are
the inductance and the capacitance per unit length of the circuit.
If "e" denotes the voltage between the wires at the point "o" of
the system, the following conditions must be satisfied if the
circuit is to oscillate at its natural frequency (the effect of
damping is here neglected):

$$e = I_2 \, j\sqrt{\tfrac{L}{C}} \, \tan l_2 \sqrt{LC}\,\omega = I_1 \, j\sqrt{\tfrac{L}{C}} \, \tan l_1 \sqrt{LC}\,\omega = -j\frac{I_0}{C_0\,\omega} \quad ;$$

$$I_1 + I_2 + I_3 = 0 .$$

Eliminating e, I_1, I_2 and I_0 from the above equations, the following relation is obtained between the constants of the circuit L, C, and C_0, the lengths L_1 and l_2 and the angular frequency :

$$C_0 \, \omega \sqrt{\frac{L}{C}} = \text{Cotan} \, l_2 \sqrt{LC} \, \omega + \text{Cotan} \, l_1 \sqrt{LC} \, \omega$$

For two parallel wires the following relations can be written:

$$\sqrt{LC} = \frac{1}{v} \; ; \quad \omega = 2\pi f = 2\pi \frac{v}{\lambda} \; ; \quad \sqrt{LC} \, \omega = \frac{2\pi f}{v} = \frac{2\pi}{\lambda}$$

$$C_0 \, \omega \sqrt{\frac{L}{C}} = \frac{C_0}{C} \, \omega \sqrt{LC} = \frac{C_0}{C} \cdot \frac{2\pi}{\lambda}$$

Hence, the natural frequency of the circuit can be determined from the following equation:

$$\text{Cotan} \, \frac{l_1}{\lambda} \, 2\pi + \text{Cotan} \, \frac{l_2}{\lambda} \, 2\pi = \frac{C_0}{C} \cdot \frac{2\pi}{\lambda} \quad \cdots \cdot (1)$$

For special cases the above formula can be somewhat simplified, as follows:

Case 1. $C_0 = 0$.

$$\text{Cotan} \, \frac{l_1}{\lambda} \, 2\pi + \text{Cotan} \, \frac{l_2}{\lambda} \, 2\pi = 0$$

$$\text{Cotan} \, \frac{l_1}{\lambda} = - \text{Cotan} \, \frac{l_2}{\lambda} \, 2\pi$$

$$\frac{l_1}{\lambda} \, 2\pi = n\pi - \frac{l_2}{\lambda} \, 2\pi \, ;$$

$$\therefore \quad l_1 + l_2 = n \frac{\lambda}{2} \quad \cdots \cdots \cdots \cdots (2)$$

Case 2. $l_1 = l_2 = 1$

$$2 \, \text{Cotan} \, \frac{l}{\lambda} \, 2\pi = \frac{C_0}{C} \cdot \frac{2\pi}{\lambda}$$

$$\therefore \quad \text{Cotan} \, \frac{l}{\lambda} \, 2\pi = \frac{C_0}{2C} \, \frac{2\pi}{\lambda} \quad \cdots \cdots (3)$$

Case 3. $l_1 + l_2 = \Lambda$ = Const.

$$Cotan \frac{l_1}{\lambda} 2\pi + Cotan \frac{\Lambda - l_1}{\lambda} 2\pi = \frac{C_o}{C} \cdot \frac{2\pi}{\lambda} \quad \cdots \cdots (4).$$

To check the application of this simple theory to the case of a tube placed in the middle of the oscillating circuit, the value of $\frac{C_o}{C}$ was calculated from the experimental results for different values of λ.

The experimental data is shown in Table I below.

TABLE I.

λ_{cm}	109	102	92	82	60	48	38	30
Λ_{cm}	40	35	30	25	46	77	58	33.5
l_{1cm}	20	17.5	15	12.5	9	26	19	16.75
l_{2cm}	20	17.5	15	12.5	37	51	39	16.75

Calculated values of $\frac{C_o}{C}$ using formula (3) for λ= 109, 102, 92, 82 and 30, and formula (1) for λ=60, 48, 38,cm., are shown in tables II, III, and IV. The values of $\frac{C_o}{C}$ are almost equal for wavelengths in the region λ = 109 to 60 cm. For shorter wavelengths the value of $\frac{C_o}{C}$ increases. This increase can not be attributed to inaccuracy of measurements but is probably due to the fact that at shorter wavelengths some factor other than the capacitance between the electrodes plays an important part, as for instance, the inductance of the grid spiral, which has been entirely neglected in the above discussion.

NOtwithstanding the fact that the theory presented above is not directly applicable to this case, the derived formulas will be used

TABLE II.

λ	$\frac{l}{\lambda}$	$\frac{l}{\lambda}2\pi$	$Cot\frac{l}{\lambda}2\pi$	$\frac{\pi}{\lambda}$	$\frac{c_0}{c}=\frac{Cot\frac{l}{\lambda}2\pi}{\pi/\lambda}$
109	.18035	66.0°	.445	.0287	15.5
102	.1715	61.7	.539	.0308	17.5
92	.1630	58.7	.609	.0340	17.9
82	.1525	54.8	.705	.0383	18.4
30	.5490	197.5	3.17	.1047	30.3

TABLE III.

λ	$\frac{l_1}{\lambda}$	$\frac{l_1}{\lambda}2\pi$	$Cot\frac{l_1}{\lambda}2\pi$	$\frac{l_2}{\lambda}$	$\frac{l_2}{\lambda}2\pi$	$Cot\frac{l_2}{\lambda}2\pi$	$Cot\frac{l_1}{\lambda}2\pi + Cot\frac{l_2}{\lambda}2\pi$	$\frac{2\pi}{\lambda}$	$\frac{c_0}{c}$
60	.150	54°	.726	.617	222°	1.110	1.836	.105	17.5
48	.542	195	3.73	1.062	383	2.35	6.08	.131	46.4
38	.500	180	∞	1.027	370	5.67	∞	.165	∞

TABLE IV.

λ	$\frac{c_0}{c}$
109	15.5
102	17.5
92	17.9
82	18.4
60	17.5
48	46.4
38	∞
30	30.3

Table V

$\frac{l_2}{\lambda}\%$	$\frac{l_2}{\lambda}2\pi$	$Cot\frac{l_2}{\lambda}2\pi$	$\frac{c_0}{c}\cdot\frac{2\pi}{\lambda}=1.0$				$\frac{c_0}{c}\cdot\frac{2\pi}{\lambda}=2.0$				$\frac{c_0}{c}\cdot\frac{2\pi}{\lambda}=5.0$				$\frac{c_0}{c}\cdot\frac{2\pi}{\lambda}=10.0$			
			$1-Cot$	$\frac{l_1}{\lambda}2\pi$	$\frac{l_1}{\lambda}\%$	$\frac{l_1+l_2}{\lambda}\%$	$2-Cot$	$\frac{l_1}{\lambda}2\pi$	$\frac{l_1}{\lambda}\%$	$\frac{l_1+l_2}{\lambda}\%$	$5-Cot$	$\frac{l_1}{\lambda}2\pi$	$\frac{l_1}{\lambda}\%$	$\frac{l_1+l_2}{\lambda}\%$	$10-Cot$	$\frac{l_1}{\lambda}2\pi$	$\frac{l_1}{\lambda}\%$	$\frac{l_1+l_2}{\lambda}\%$
50	3.14	$-\infty$	$+\infty$	0	0	50.0	$+\infty$	0	0	50.0	$+\infty$	0	0	50.0	$+\infty$	0	0	50.0
40	2.51	-1.376	2.376	.398	6.34	46.34	3.376	.288	4.58	44.58	6.376	.155	2.47	42.47	11.376	.088	1.40	41.4
30	1.88	-.325	1.325	.646	10.3	40.3	2.325	.407	6.47	36.47	5.325	.185	2.95	32.95	10.326	.097	1.54	31.54
25	1.57	0	1.00	.785	12.5	37.5	2.000	.462	7.33	32.33	5.000	.196	3.12	28.12	10.000	.099	1.57	26.57
20	1.257	.325	+.675	.977	15.5	35.5	1.675	.538	8.55	28.55	4.675	.210	3.35	23.35	9.675	.102	1.62	21.62
15	.942	.726					1.274	.666	10.6	25.60	4.274	.230	3.66	18.66	9.274	.107	1.70	16.70
10	.628	1.376									3.624	.268	4.27	14.27	8.624	.114	1.82	11.22
5	.314	3.077													6.923	.143	2.28	7.28
						min. 35.2				min. 25.00				min. 12.10				min. 6.32

to find how much the natural frequency of the system changes if the condenser C_0 is displaced from the middle position.

First, the relation between L_1 and l_2 will be found for the case $l_1 \neq l_2$ and $\lambda = $ const. This can be found from formula (1), p. 23. The results are shown in Tables V and VI, and are represented graphically on Diagram 7. In general, it can be said, that the sum $l_1 + l_2$ is greater when $l_1 \neq l_2$ than when $l_1 = l_2$.

In the experiments of this thesis, the value of $(l_1 + l_2)$ has been kept constant. Let us find how much the wavelength will be changed if the condenser C_0 is displaced from the central position. Formula (1) can be written as follows:

$$Cotan\left(\frac{l_o}{\lambda}2\pi + \frac{\Delta l_o}{\lambda}2\pi\right) + Cotan\left(\frac{l_o}{\lambda}2\pi - \frac{\Delta l_o}{\lambda}2\pi\right) = \frac{C_o}{C}\cdot\frac{2\pi}{\lambda}$$

where $l_1 = l_o + \Delta l_o$ and $l_2 = l_o - \Delta l_o$, so that $l_1 + l_2 = 2l_o = $ const. The values of $Cotan\frac{l}{\lambda}2\pi$, $2 \times Cotan\frac{l}{\lambda}2\pi$ and the sum $Cot\frac{l+\Delta l}{\lambda}2\pi + Cot\frac{l-\Delta l}{\lambda}2\pi$ are plotted as functions of $\frac{l}{\lambda}$ on Diagram 8. If λ_o is the wavelength corresponding to the case $l_1 = l_2$ (or $\Delta l_o = 0$), then for a given value of $\frac{C_o}{C}\cdot\frac{2\pi}{\lambda_o} = \alpha_o$, we can find the value of $\frac{l_o}{\lambda} = \beta_o$ from the condition that $2Cot\frac{l_o}{\lambda}2\pi = \alpha_o$. Now, if we make $l_1 = l_0 + \Delta l_0$, and $l_2 = l_0 - \Delta l_0$, the value of λ_o will change to λ and α_o will change to α so that $\frac{\alpha}{\alpha_o} = \frac{\lambda_o}{\lambda}$. The corresponding value of β will be: $\beta = \beta_o\frac{\alpha}{\alpha_o}$. Knowing the value of β we can find from curves on Dia.8 the value of $\frac{l_1}{\lambda}$, and then the value of $\frac{\Delta l}{\lambda} = \frac{l_1}{\lambda} - \beta$. We want to express Δl in terms of the original wavelength λ_o; this can be done as follows: $\frac{\Delta l_o}{\lambda_o} = \frac{\Delta l_o}{\lambda}\cdot\frac{\lambda}{\lambda_o} = \frac{\Delta l_o}{\lambda}\cdot\frac{\alpha}{\alpha_o}$.

Thus assuming the value of α, we can find the value of the displacement Δl_o. By this method the table VII has been computed and

TABLE VI.

$\frac{c_o}{c} \cdot \frac{2\pi}{\lambda}$	$Cot\frac{\ell}{\lambda}2\pi$	$\frac{\ell}{\lambda}2\pi$	$\frac{\ell}{\lambda}$
0.0	.0	1.57	.250
.2	.1	1.475	.234
.4	.2	1.370	.218
.6	.3	1.280	.204
.8	.4	1.190	.189
1.0	.5	1.107	.176
1.2	.6	1.029	.164
1.4	17	.960	.153
1.6	.8	.896	.142
1.8	.9	.838	.133
2.0	1.0	.785	.125
2.5	1.25	.675	.107
3.0	1.50	.587	.0935
3.5	1.75	.518	.0826
4.0	2.00	.462	.0733
4.5	2.25	.419	.0668
5.0	2.50	.380	.0605
6.0	3.0	.320	.0508
7.0	3.5	.277	.0440
8.0	4.0	.244	.0388
9.0	4.5	.218	.0347
10.0	5.0	.198	.0316

Diagram 8.

$$Cot \frac{l+\Delta l}{\lambda} 2\pi + Cot \frac{l-\Delta l}{\lambda} 2\pi$$

$2 Cotan \frac{l}{\lambda} 2\pi$

$Cotan \frac{l}{\lambda} 2\pi$

6.0
5.5
5.0
4.5
4.0
3.5
3.0
2.5
2.0
1.5
1.0
.5
0
.5
1.0
1.5
2.0
2.5
3.0

.05   .10   .15   .20   .25   .30   .35   .40   .45   .50

$\longrightarrow \frac{l}{\lambda}$

TABLE VII. (30)

α'	$\dfrac{\alpha_0}{\alpha'}=\dfrac{\lambda'}{\lambda_0}$	$\beta'\approx\beta_0\dfrac{\alpha'}{\alpha_0}$	$\dfrac{\ell'}{\lambda'}$	$\dfrac{\Delta\ell}{\lambda'}$	$\dfrac{\Delta\ell_0}{\lambda_0}=\dfrac{\Delta\ell}{\lambda'}\cdot\dfrac{\alpha'}{\alpha_0}$	
1.05	.953	.1858	.255	.069	6.58	
1.10	.909	.195	.285	.090	8.17	$\alpha_0=\dfrac{C_0}{C}\cdot\dfrac{2\pi}{\lambda_0}=1.0$
1.15	.870	.204	.310	.106	9.22	
1.177	.850	.208	.333	.121	10.30	$\beta_0=\dfrac{\ell_0}{\lambda_0}=1.77$
1.25	.800	.221	.380	.159	12.70	
1.33	.750	.236	.430	.194	14.50	
1.41	.707	.250	.500	.250	17.70	
2.11	.95	.132	.171	.059	5.60	
2.22	.90	.139	.209	.070	6.30	
2.35	.85	.147	.225	.078	6.63	$\alpha_0=2.0$
2.50	.80	.156	.255	.099	7.90	
2.86	.70	.178	.313	.131	9.16	$\beta_0=.125$
3.34	.60	.208	.380	.172	10.30	
4.00	.50	.250	.500	.250	12.50	
3.16	.95	.098	.126	.028	2.66	
3.34	.90	.103	.148	.045	4.05	
3.54	.85	.109	.168	.059	5.00	$\alpha_0=3.0$
3.75	.80	.116	.187	.071	5.68	
4.28	.70	.133	.233	.100	7.00	$\beta_0=.093$
5.00	.60	.155	.285	.130	7.80	
6.00	.50	.186	.351	.165	8.25	

Diagram 9.
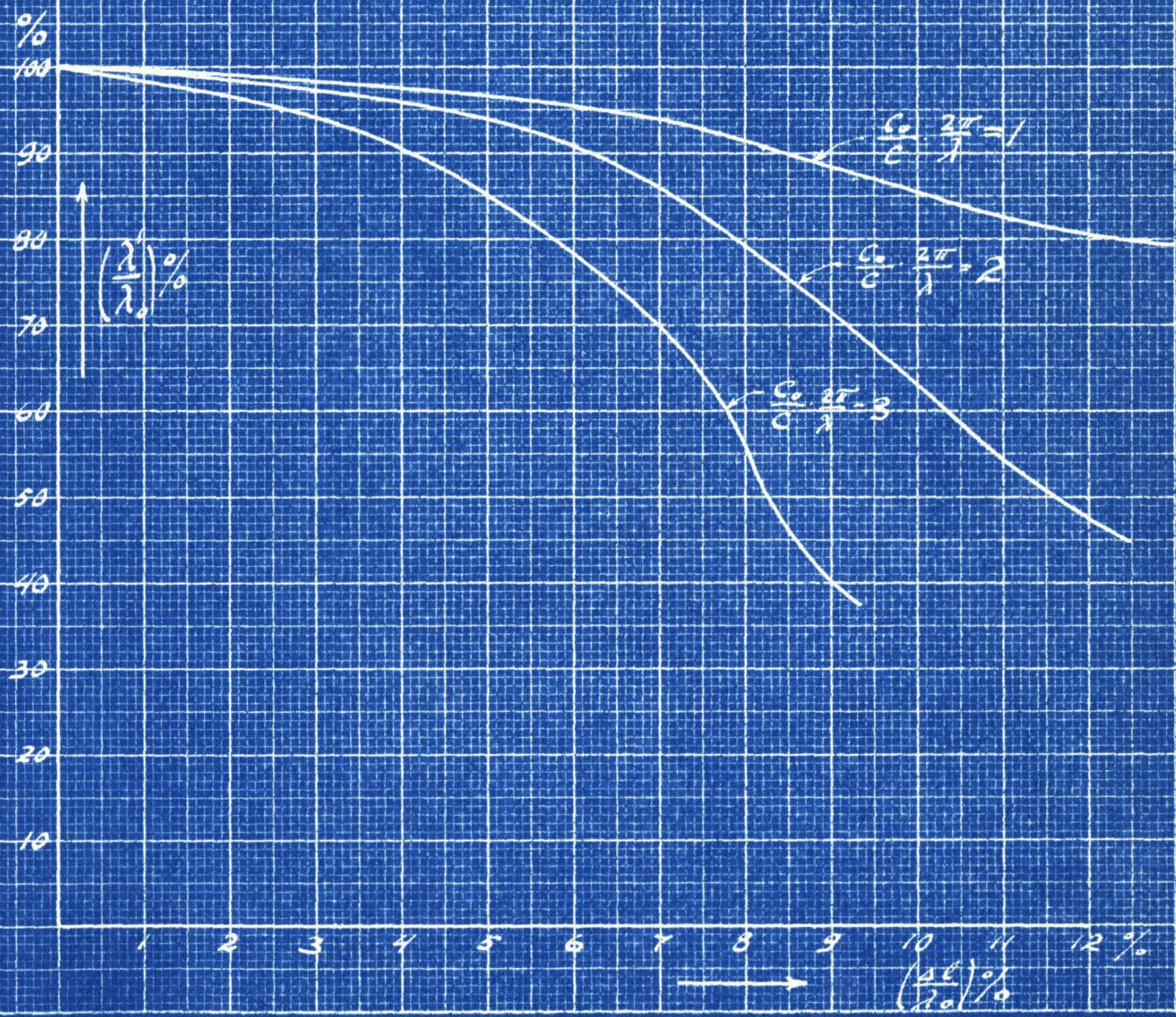
the curves on Diagram 9 represent the change of wavelength $\frac{\lambda}{\lambda_o}$ with the displacement $\frac{\Delta l_o}{\lambda_o}$ for the condition $l_1 + l_2 =$ const. For large values of $\frac{C_o}{C} \cdot \frac{2\pi}{\lambda_o}$ the calculated values of the wavelengths decrease quite rapidly with the displacement.

The experimental results, however, show that the wavelength is increasing slightly instead of decreasing when the electrodes are displaced from the central position. This effect can be explained only by the presence of inductance as well as capacitance in the middle of the circuit. This inductance is evidently the inductance of the grid spiral, and its effect will be considered in the next paragraph.

(d). Effect of lumped inductance in the Lecher system.

If inductances L_0 (see Fig.7) are placed in each wire of a short circuited Lecher system, the natural frequency of the circuit
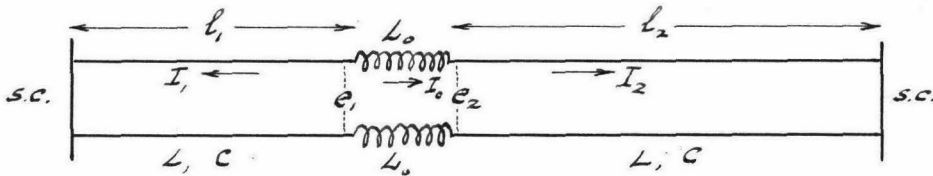

Fig. 7.

can be found from the following conditions:

$$e_1 = I_1 \, j \sqrt{\tfrac{L}{C}} \, \tan l_1 \sqrt{LC} \, \omega$$

$$e_2 = I_2 \, j \sqrt{\tfrac{L}{C}} \, \tan l_2 \sqrt{LC} \, \omega$$

$$e_1 - e_2 = j \, I_o \, 2L_o \, \omega$$

$$I_2 = I_o ; \quad I_1 = -I_o$$

$$\therefore \; I_1 \, j \sqrt{\tfrac{L}{C}} \, \tan l_1 \sqrt{LC} \, \omega - I_2 \, j \sqrt{\tfrac{L}{C}} \, \tan l_2 \sqrt{LC} \, \omega = j \, I_o \, 2L_o \, \omega$$

$$I_1 \, j \sqrt{\tfrac{L}{C}} \, \tan l_1 \sqrt{LC} \, \omega = - I_1 \, j \sqrt{\tfrac{L}{C}} \, \tan l_2 \sqrt{LC} \, \omega - j \, I_1 \, 2L_o \, \omega$$

$$\text{or:}\quad \tan \ell_1 \sqrt{LC}\,\omega + \tan \ell_2 \sqrt{LC}\,\omega = -2L_0\,\omega\sqrt{\frac{C}{L}}$$

$$\text{or:}\quad \tan \frac{\ell_1}{\lambda}2\pi + \tan \frac{\ell_2}{\lambda}2\pi = -\frac{2L_0}{L}\cdot\frac{2\pi}{\lambda} \quad \ldots\ldots (6)$$

$$\text{If:}\quad \ell_1 = \ell_2 :$$

$$\tan \frac{\ell_1}{\lambda}2\pi = -\frac{L_0}{L}\cdot\frac{2\pi}{\lambda}$$

(d). Effect of a circuit of length l_0, having distributed capacitance C_0 and the inductance L_0 per unit length, placed in the Lecher system.

The circuit is represented in Fig.8.
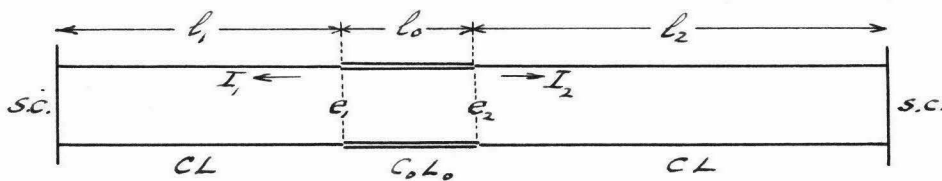
Fig. 8.

The following equations can be used to find the natural frequency of the circuit:

$$e_1 = I_1\, j\sqrt{\frac{L}{C}}\,\tan \ell_1 \sqrt{LC}\,\omega \quad \ldots\ldots (7)$$

$$e_2 = I_2\, j\sqrt{\frac{L}{C}}\,\tan \ell_2 \sqrt{LC}\,\omega \quad \ldots\ldots (8)$$

$$e_2 = e_1\, \cos \ell_0 \sqrt{L_0 C_0}\,\omega + j I_1 \sqrt{\frac{L_0}{C_0}}\,\sin \ell_0 \sqrt{L_0 C_0}\,\omega \quad \ldots\ldots (9)$$

$$e_1 = e_2\, \cos \ell_0 \sqrt{L_0 C_0}\,\omega + j I_2 \sqrt{\frac{L_0}{C_0}}\,\sin \ell_0 \sqrt{L_0 C_0}\,\omega \quad \ldots\ldots (10)$$

Substituting (7) and (8) into (9) and (10):

$$I_2\, j\sqrt{\frac{L}{C}}\,\tan \ell_2 \sqrt{LC}\,\omega = I_1\, j\sqrt{\frac{L}{C}}\,\tan \ell_1 \sqrt{LC}\,\omega\,\cos \ell_0 \sqrt{L_0 C_0}\,\omega + j I_1 \sqrt{\frac{L_0}{C_0}}\,\sin \ell_0 \sqrt{L_0 C_0}\,\omega \ldots (11)$$

$$I_1\, j\sqrt{\frac{L}{C}}\,\tan \ell_1 \sqrt{LC}\,\omega = I_2\, j\sqrt{\frac{L}{C}}\,\tan \ell_2 \sqrt{LC}\,\omega\,\cos \ell_0 \sqrt{L_0 C_0}\,\omega + j I_2 \sqrt{\frac{L_0}{C_0}}\,\sin \ell_0 \sqrt{L_0 C_0}\,\omega \ldots (12)$$

or, $\quad I_2 \tan l_2 \sqrt{LC}\,\omega = I_1\left\{\tan l_1 \sqrt{LC}\,\omega \cos l_0\sqrt{L_0 C_0}\,\omega + \sqrt{\dfrac{L_0 C}{C_0 L}}\sin l_0 \sqrt{L_0 C_0}\,\omega\right\} \cdots (13)$

$I_1 \tan l_1 \sqrt{LC}\,\omega = I_2\left\{\tan l_2 \sqrt{LC}\,\omega \cos l_0\sqrt{L_0 C_0}\,\omega + \sqrt{\dfrac{L_0 C}{C_0 L}}\sin l_0 \sqrt{L_0 C_0}\,\omega\right\} \cdots (14)$

Eliminating I_1 and I_2 from (13) and (14) we get the following relation between the constants of the circuit and the frequency:

$$\tan l_1 \sqrt{LC}\,\omega \tan l_2 \sqrt{LC}\,\omega = \tan l_1 \sqrt{LC}\,\omega \tan l_2 \sqrt{LC}\,\omega \cos^2 l_0 \sqrt{L_0 C_0}\,\omega \;+$$

$$\dfrac{L_0 C}{C_0 L}\sin^2 l_0 \sqrt{L_0 C_0}\,\omega + \left\{\tan l_1\sqrt{LC}\,\omega + \tan l_2 \sqrt{LC}\,\omega\right\}\sin l_0 \sqrt{L_0 C_0}\,\omega \cos l_0 \sqrt{L_0 C_0}\,\omega \cdot \sqrt{\dfrac{L_0 C}{C_0 L}} \;\cdots (15)$$

or, $\quad \tan \dfrac{l_1}{\lambda} 2\pi \tan \dfrac{l_2}{\lambda} 2\pi \left\{1 - \cos^2 l_0 \sqrt{L_0 C_0}\,\omega\right\} = \dfrac{L_0 C}{C_0 L}\sin^2 l_0 \sqrt{L_0 C_0}\,\omega \;+$

$$+ \sqrt{\dfrac{L_0 C}{C_0 L}}\sin l_0 \sqrt{L_0 C_0}\,\omega \cos l_0 \sqrt{L_0 C_0}\,\omega \left\{\tan \dfrac{l_1}{\lambda} 2\pi + \tan \dfrac{l_2}{\lambda} 2\pi\right\}$$

$$\left\{\tan \dfrac{l_1}{\lambda} 2\pi \tan \dfrac{l_2}{\lambda} 2\pi - \dfrac{L_0 C}{C_0 L}\right\}\sin^2 l_0 \sqrt{L_0 C_0}\,\omega = \sqrt{\dfrac{L_0 C}{C_0 L}}\sin l_0 \sqrt{L_0 C_0}\,\omega \cos l_0 \sqrt{L_0 C_0}\,\omega \;\cdot$$

$$\cdot \left\{\tan \dfrac{l_1}{\lambda} 2\pi + \tan \dfrac{l_2}{\lambda} 2\pi\right\} \cdot$$

$$\therefore \quad \tan l_0 \sqrt{L_0 C_0}\,\omega = \sqrt{\dfrac{L_0 C}{C_0 L}}\; \dfrac{\tan \dfrac{l_1}{\lambda} 2\pi + \tan \dfrac{l_2}{\lambda} 2\pi}{\tan \dfrac{l_1}{\lambda} 2\pi \tan \dfrac{l_2}{\lambda} 2\pi - \dfrac{L_0 C}{C_0 L}} \quad \cdots (17)$$

To check the correctness of this formula, we will consider several special cases and compare the results with formulas derived in the preceding paragraphs.

Case 1. $\quad L_0 = 0. \qquad \tan l_0 \sqrt{L_0 C_0}\, \omega = 0$

$$\tan \frac{l_1}{\lambda} 2\pi + \tan \frac{l_2}{\lambda} 2\pi = \tan \frac{l_1}{\lambda} 2\pi \tan \frac{l_2}{\lambda} 2\pi \cdot \lim \left[\frac{\tan l_0 \sqrt{L_0 C_0}\, \omega}{\sqrt{\frac{L_0 C}{C_0 L}}} \right]_{L_0 \to 0} - \lim \left[\sqrt{\frac{L_0 C}{C_0 L}} \tan l_0 \sqrt{L_0 C_0}\, \omega \right]_{L_0 \to 0}$$

$$\lim \left[\frac{\tan l_0 \sqrt{L_0 C_0}\, \omega}{l_0 \sqrt{L_0 C_0}\, \omega} \right]_{L_0 \to 0} \times \frac{l_0 C_0\, \omega}{\sqrt{\frac{C}{L}}} = l_0 C_0\, \omega \sqrt{\frac{C}{L}}$$

$$\therefore\ \tan \frac{l_1}{\lambda} 2\pi + \tan \frac{l_2}{\lambda} 2\pi = l_0 C_0 \sqrt{\frac{C}{L}}\, \omega \tan \frac{l_1}{\lambda} 2\pi \tan \frac{l_2}{\lambda} 2\pi\ ,\ or$$

$$Cotan \frac{l_1}{\lambda} 2\pi + Cotan \frac{l_2}{\lambda} 2\pi = \frac{l_0 C_0}{C} \cdot \frac{2\pi}{\lambda} \dots \dots \dots (18)$$

This is equivalent to formula (1) on p.23, where the total capacitance $l_0 C_0$ was denoted by C_0

Case 2. $\quad C_0 = 0$.

$$\tan \frac{l_1}{\lambda} 2\pi + \tan \frac{l_2}{\lambda} 2\pi = \left| \frac{\tan l_0 \sqrt{L_0 C_0}\, \omega}{\sqrt{\frac{L_0 C}{C_0 L}}} \left(\tan \frac{l_1}{\lambda} 2\pi \tan \frac{l_2}{\lambda} 2\pi \right) - \sqrt{\frac{L_0 C}{C_0 L}} \tan l_0 \sqrt{L_0 C_0}\, \omega \right|_{C_0 \to 0} =$$

$$= -\lim \left| \frac{\tan l_0 \sqrt{L_0 C_0}\, \omega}{l_0 \sqrt{L_0 C_0}\, \omega} \right|_{C_0 \to 0} \times l_0 \sqrt{L_0 C_0}\, \omega \sqrt{\frac{L_0 C}{C_0 L}} = - \frac{l_0 L_0}{L} \cdot \frac{2\pi}{\lambda}$$

$$\therefore\ \tan \frac{l_1}{\lambda} 2\pi + \tan \frac{l_2}{\lambda} 2\pi = - \frac{l_0 L_0}{L} \cdot \frac{2\pi}{\lambda} \dots \dots (19)$$

This is equivalent to formula (6), p.33, where $2L_0$, the total inductance is equivalent to $l_0 L_0$ in formula (19).

A case of particular interest to us is the following.

Case 3. $l_1 = l_2$

$$\tan l_0 \sqrt{L_0 C_0}\, \omega = \sqrt{\frac{L_0 C}{C_0 L}} \cdot \frac{2 \tan l_1 \sqrt{LC}\, \omega}{\tan^2 l_1 \sqrt{LC}\, \omega - \frac{L_0 C}{C_0 L}}$$

$$\tan^2 l_1 \sqrt{LC}\, \omega - \frac{2\sqrt{\frac{L_0 C}{C_0 L}}}{\tan l_0 \sqrt{L_0 C_0}\, \omega} \tan l_1 \sqrt{LC}\, \omega - \frac{L_0 C}{C_0 L} = 0$$

$$\therefore \ \tan l_1 \sqrt{LC}\, \omega = \frac{\sqrt{\frac{L_0 C}{C_0 L}}}{\tan l_0 \sqrt{L_0 C_0}\, \omega} \pm \sqrt{\frac{\frac{L_0 C}{C_0 L}}{\tan^2 l_0 \sqrt{L_0 C_0}\, \omega} + \frac{L_0 C}{C_0 L}} =$$

$$= \frac{\sqrt{\frac{L_0 C}{C_0 L}}}{\tan l_0 \sqrt{L_0 C_0}\, \omega} \left\{ 1 \pm \sqrt{1 + \tan^2 l_0 \sqrt{L_0 C_0}\, \omega} \right\} = \sqrt{\frac{L_0 C}{C_0 L}} \left\{ \frac{1 \pm \frac{1}{\cos l_0 \sqrt{L_0 C_0}\, \omega}}{\tan l_0 \sqrt{L_0 C_0}\, \omega} \right\} =$$

$$= \sqrt{\frac{L_0 C}{C_0 L}} \left\{ \cot an\, l_0 \sqrt{L_0 C_0}\, \omega \pm \csc l_0 \sqrt{L_0 C_0}\, \omega \right\}$$

$$\therefore \ \tan l_1 \sqrt{LC}\, \omega = \begin{cases} -\sqrt{\frac{L_0 C}{C_0 L}} \tan \frac{l_0}{2} \sqrt{L_0 C_0}\, \omega \ ; \quad \text{holds to the limit when } C_0 \to 0 \\ \text{or} \\ +\sqrt{\frac{L_0 C}{C_0 L}} \cot an \frac{l_0}{2} \sqrt{L_0 C_0}\, \omega \ ; \quad \text{holds to the limit when } L_0 \to 0 \end{cases}$$

Note: $\overleftrightarrow{\cot x - \csc x = \frac{\cos x - 1}{\sin x} = -\frac{2 \sin^2 \frac{x}{2}}{2 \sin \frac{x}{2} \cos \frac{x}{2}} = -\tan \frac{x}{2}}$

$$\cot x + \csc x = \frac{\cos x + 1}{\sin x} = \frac{2 \cos^2 \frac{x}{2}}{2 \sin \frac{x}{2} \cos \frac{x}{2}} = +\cot an \frac{x}{2}$$

$$\overleftrightarrow{\ }$$

$$\therefore \ \tan \frac{l}{\lambda} 2\pi = \begin{cases} -\sqrt{\frac{L_0 C}{C_0 L}} \tan \frac{l_0}{2} \sqrt{L_0 C_0}\, \omega \quad \ldots \ldots (20) \\ \text{or} \\ +\sqrt{\frac{L_0 C}{C_0 L}} \cot an \frac{l_0}{2} \sqrt{L_0 C_0}\, \omega \ldots \ldots (21) \end{cases}$$

Now, using equation (21) let us calculate the value of $\sqrt{\frac{L_0 C}{C_0 L}}$ from the experimental data shown in Table I, p.24, and then compare it with the theoretical value calculated from the dimensions of the circuit.

To do this, let us rewrite equation (21) in the following form:

$$\sqrt{\frac{L_0 C}{C_0 L}} \; \text{Cotan} \frac{\ell_0}{2} \sqrt{L_0 C_0} \; \frac{2\pi}{\lambda} v = \tan \frac{\ell}{\lambda} 2\pi \; \dots \dots (21)'$$

where "v" is the velocity of propagation of waves along the parallel wires (very nearly equal to the velocity of light if the damping is small). Denote the value $\frac{\ell_0}{2} \sqrt{L_0 C_0} \, 2\pi v = \alpha$, then:

$$\sqrt{\frac{L_0 C}{C_0 L}} \; \text{Cotan} \frac{\alpha}{\lambda} = \tan \frac{\ell}{\lambda} 2\pi \; \dots \dots (22)$$

If we know "l" and "λ" for two different wavelengths, then:

$$\frac{\text{Cotan} \frac{\alpha}{\lambda'}}{\text{Cotan} \frac{\alpha}{\lambda''}} = \frac{\tan \frac{\ell'}{\lambda'} 2\pi}{\tan \frac{\ell''}{\lambda''} 2\pi} \; \dots \dots (23)$$

from which "x" can be calculated, and then, if the value of "x" is substituted into (22), the value of $\sqrt{\frac{L_0 C}{C_0 L}}$ can be calculated. However, this method is not accurate, because a small error in measurements of "l" or "λ" will result in a considerable error in "x". We will use another method. We know that for $\lambda = 30$ cm., $l \approx 0$; hence we can write from equation (22):

$$\text{Cotan} \frac{\alpha}{\lambda} = 0; \quad x = 1.57 \lambda \approx 1.57 \times 30 = 47.2$$

Using this value of "x" the value of $\sqrt{\frac{L_0 C}{C_0 L}}$ has been calculated by means of equation (22). The results are shown in Table VIII, p.38. The average value of $\sqrt{\frac{L_0 C}{C_0 L}}$ is about 0.80.

Let us now calculate the value of $\sqrt{\frac{L_0 C}{C_0 L}}$ from the dimensions of the circuits (see Fig.9 and Fig.10).

TABLE VIII.

λ	109	102	92	82	60	48	30
ℓ	18.7	16.2	13.7	11.2	6.5	3.0	0
$\frac{\ell}{\lambda}2\pi$	1.08	.998	.937	.859	.680	.393	0
$\tan\frac{\ell}{\lambda}2\pi$	1.868	1.55	1.36	1.16	.809	.414	0
$\frac{x}{\lambda}$	.43	.462	.513	.576	.785	.983	1.57
$\cot an\frac{x}{\lambda}$	2.17	2.00	1.77	1.54	1.00	.666	0
$\sqrt{\frac{L_0 C}{C_0 L}}$	.86	.775	.768	.755	.809	.620	

For two parallel wires, the capacitance and the inductance

per unit length are found from the following formulae:

$d = 2.7$ cm.

$r = .3$ cm.
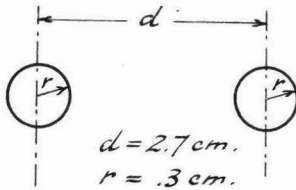
Fig. 9.

$$C = \frac{\pi p}{\log \frac{d}{r}} \quad \dots \quad (24)$$

$$L = \frac{\mu}{\pi} \log \frac{d}{r} \quad \dots \quad (25)$$

where $p \approx 8.85 \times 10^{-14}$ and $\mu = 0.4 \times 10^{-8}$.

Substituting the above figures and the dimensions of the circuit

in formulas (24) and (25), we find:

$$C = \frac{\pi \times 8.85 \times 10^{-14}}{\log \frac{2.7}{.3}} = 12.65 \times 10^{-14} \frac{far}{cm.}$$

$$L = \frac{.4 \pi \times 10^{-8}}{\pi} \log \frac{2.7}{.3} = .88 \times 10^{-8} \frac{henry}{cm.}$$

To check:

$$\frac{1}{\sqrt{LC}} = \frac{1}{\sqrt{12.65 \times .88 \times 10^{-22}}} = 3 \times 10^{10} \frac{cm}{sec.} \quad (O.K).$$

The grid to plate capacitance can be calculated approximately

if we assume that the plate and the grid form a cylindrical
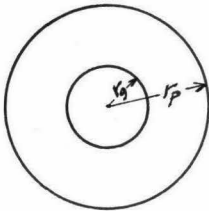
condenser of radii r_p and r_g. Then:

$\frac{r_p}{r_g} = 3.5$

Fig. 10.

$$C_o = \frac{2\pi p}{\log \frac{r_p}{r_g}} = \frac{2\pi \times 8.85 \times 10^{-14}}{\log 3.5} = 44.5 \times 10^{-14} \frac{far.}{cm} \dots (26).$$

Since the length of the plate is

equal to $l_o \approx 2.6$ cm., this gives as

the total grid to plate capacitance:

$$C_o l_o = 115 \times 10^{-14} \text{ farads, and}$$

the ratio $\frac{C_o l_o}{C}$ becomes equal to: $\frac{C_o l_o}{C} = \frac{115 \times 10^{-14}}{12.65 \times 10^{-14}} = 9.1$.

However, the experimental results interpreted on the basis of

the assumption that the grid inductance is negligible, which is valid for long wavelengths, gave the value of $\frac{C_0 l_0}{C} = 18$. Therefore we will take C_O equal to:

$$C_O \approx 90 \times 10^{-14} \text{ far./cm.}$$

<u>Note:</u> Formula (24) gives the value of C_O too small because it neglects the end effects, which tend to increase the capacitance.

To calculate the effective inductance of the grid spiral accurately is difficult, because it can not be treated as an ordinary inductance, since the current is different in different parts of the grid. When the loop of the voltage wave coincides with the center of the grid, the current is positive in one half of the grid and negative in the other, thus the effective inductance of the grid spiral is diminished (see Fig.11). It seems reasonable, then, to take as the value of the inductance of the grid per unit length the inductance of one turn times the number of turns per cm.

$$I \leftarrow \qquad \rightarrow I$$
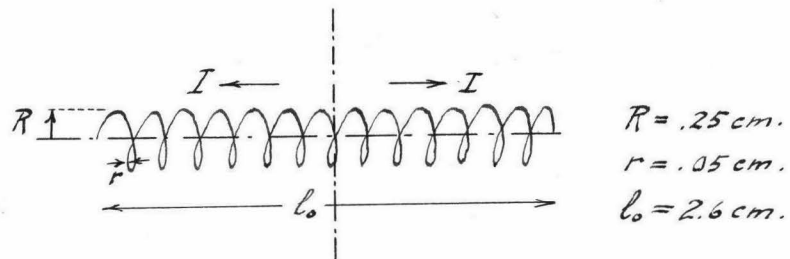
$$R = .25 \, cm.$$
$$r = .05 \, cm.$$
$$l_o = 2.6 \, cm.$$

Fig. 11.

The inductance of a single turn of radius R of wire of radius r, is expressed by the formula:

$$L_1 = 4\pi R\left[\left(1+\frac{r^2}{8R^2}\right)\log\frac{8R}{r}+\frac{r^2}{24R^2} - 1.75\right] \quad \text{cm.} \quad \ldots\ldots(27)$$

Or, since the value of r^2/R^2 is small:

$$L_1 \approx 4\pi R\left[\log\frac{8R}{r} - 1.75\right] \quad \times 10^{-9} \text{ henry} \quad \ldots\ldots(27)'$$

Substituting the values of R = .25 cm. and r = .05 cm., we get:

$$L_1 = 4\pi \times .25 \left[\log \frac{8 \times .25}{.05} - 1.75 \right] = \sim 6 \text{ cm.} = 6 \times 10^{-9} \text{ henry/turn.}$$

The grid has 10 turns per cm., so the inductance of the grid per centimeter: $L = 6 \times 10^{-8}$ henry/cm. In the above theory a symmetrical circuit has been assumed. Therefore we must take as the value of the inductance per unit length of the circuit l_0 (Fig.8),

$$L_0 = L/2 = 3 \times 10^{-8} \text{ henry/cm.}$$

Using the values of L, C, L_0 and C_0 calculated above, we find:

$$\sqrt{\frac{L_0 C}{C_0 L}} = \sqrt{\frac{3 \times 10^{-8} \times 12.65 \times 10^{-14}}{.88 \times 10^{-8} \times 90 \times 10^{-14}}} = \sim .694.$$

Considering the roughness of approximations made in deriving this value, the agreement with the experimental value (0.8) is surprizingly good. The value of $x = \frac{l_0}{2} \sqrt{L_0 C_0} \cdot 2\pi \nu$ (see p.37) for the above values of L, C, L_0 and C_0, becomes:

$$x' = \frac{2.6}{2} \times 2\pi \times 3 \times 10^{10} \sqrt{3 \times 10^{-8} \times 90 \times 10^{-14}} = 40.2$$

The value found on p.37 was $x = 47.2$. The ratios:

$$\frac{x}{x'} = \frac{47.2}{40.2} = 1.17 \quad \text{and} \quad \frac{\left(\sqrt{\frac{L_0 C}{C_0 L}} \right)_{exp.}}{\left(\sqrt{\frac{L_0 C}{C_0 L}} \right)_{theor.}} = \frac{.80}{.69} = 1.15$$

indicate that the true value of L_0 must be:

$$L_0 \approx 3 \times 10^{-8} \times (1.16)^2 = 4 \times 10^{-8} \text{ henry/cm.}$$

The above presented analysis gives the explaination why
the natural frequency of the circuit remained constant when the
tube was displaced from the central position: the inductance of
the grid neutralized the effect of the grid to plate capacity.
Analyzing the distribution of standing waves on the wires, shown
on p.21, it can be concluded that when the frequency approached
$\lambda \approx 30$ cm. the effective length of the grid was equal to half
wavelength. For this wavelength, then, the A.C. voltage amplitude
was different for different positions along the grid. The average
value of the voltage amplitude on the grid was less than its
maximum value, while for longer wavelengths the A.C. voltage was
very nearly the maximum throughout the length of the grid. Since
the A.C. grid to plate voltage is the factor which produces
oscillations of the space charge which supplies its energy to
the oscillating circuit, the rapid increase of the minimum grid
current when the wavelength approached $\lambda \approx 30$ cm., can be
under-stood. A short circuited grid as a remedy for this
undesirable phenomenon, was mentioned on p. 18.

Comparing the circuit shown in Fig.4, which can be called
the "double" circuit, with the circuit shown in Fig.1, it can be
said, that the average grid to plate voltage will be higher for
the"double" circuit than for the"single" circuit, which will
result in a greater amplitude of oscillations for the same grid
current for the double circuit. Another advantage in the use of
this circuit is the possibility of studying the distribution
of standing waves along the electrodes, which will aid in the study

of the mechanism of the generation of Barkhausen oscillations.
It also gives a simple method for the suppression of normal
waves when shorter waves of higher order only are desired.

5. Wavelength measurements.

The first evidence of the presence of oscillations in the
circuit is the appearance of the plate current. This current flows
in the direction such as to charge the negative plate battery. This
can happen only if the electrons gain more energy in the space
filament-grid than what they loose in their path from grid to plate.
If there were no oscillations the energy on the two sides is the
same and consequently no plate current flows. If the bridge "B" (F.1)
is moved along the wires while the grid potential is kept constant,
the grid current will be a maximum when the natural frequency of
the circuit corresponds to the electronic frequency or its multiple.
The distance along the wires between the maxima of the plate current
will be then equal to one half wavelength. This is one of the most
convenient methods of measuring the wavelength. If the plate current
is plotted as a function of the position of the bridge, as shown on
Diagram 10, and the wavelength is determined from the curve, the
accuracy of this method is quite high (a few millimeters).

The above described method was used together with another, which
consisted in bringing close to the oscillating circuit an auxiliary
Lecher system. When the natural frequency of the auxiliary system was
the same as that of the first circuit, a decrease of the plate current
was observed, because the auxiliary circuit then absorbed energy from
the primary circuit.

Diagram 10.

Change of plate current with
displacement of the bridge.

$E_h = Const.$
$I_h = Const.$
$E_g = Const.$
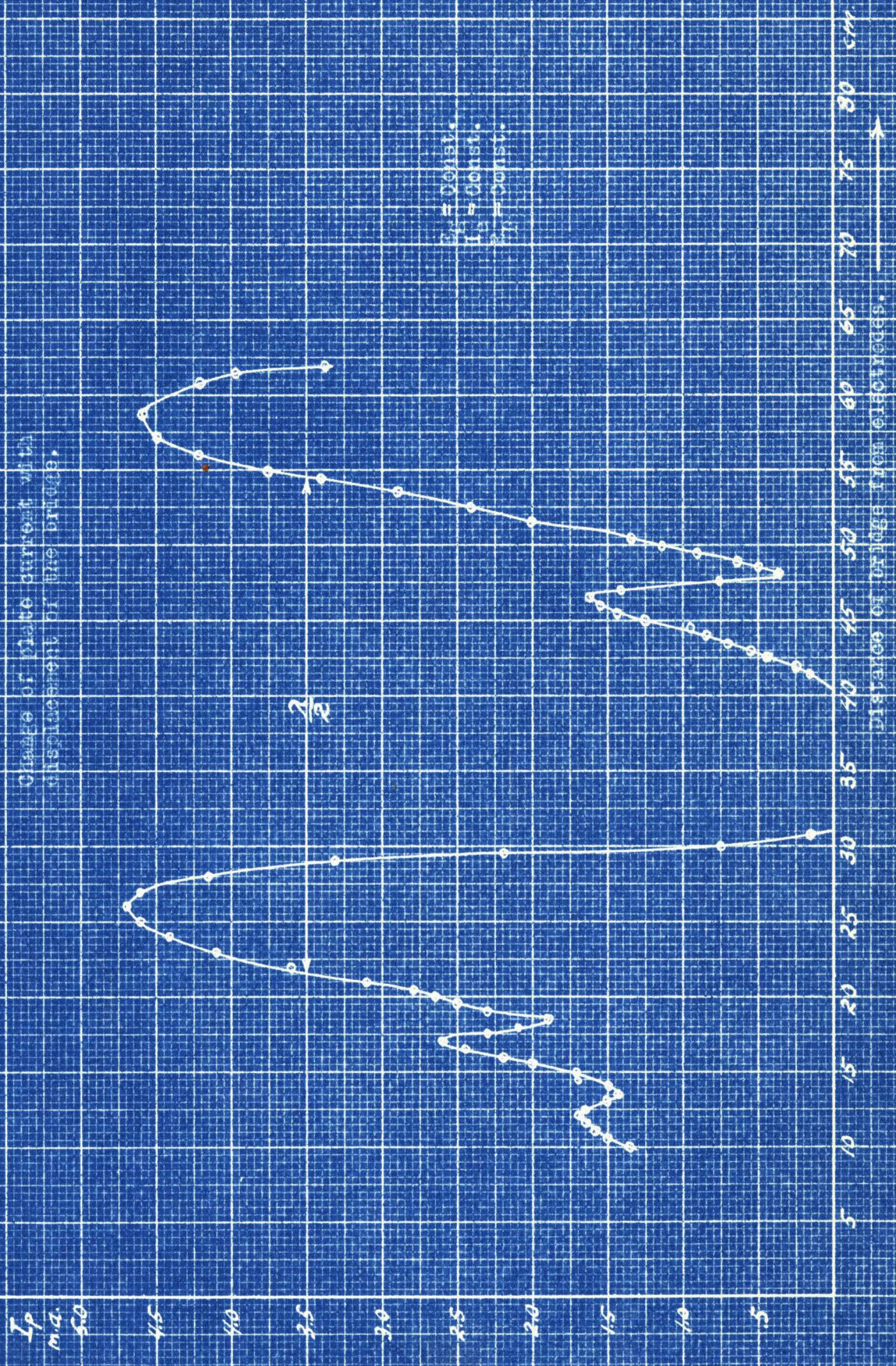
For small amplitudes of oscillations the frequency of the circuit for maximum output was found to correspond to the theoretical value of the electronic frequency or its multiple, calculated from the dimensions of the tube. Scheibe's formula (Ref.12) for cylindrical electrodes was used for calculating the wavelength:

$$\lambda = \frac{1000\, d_g\,(cm)}{\sqrt{E_g\,(volts)}} \left\{ f\left(\sqrt{\ln \frac{r_g}{r_f}}\right) + g\left(\sqrt{\frac{E_f}{E_g - E_p}\, \ln \frac{r_p}{r_g}}\right) \right\} \quad cm.$$

where: $f\left(\sqrt{\ln \frac{r_g}{r_f}}\right) = f(x) = x e^{-x^2} \int_0^x e^{u^2} du,\; u = \sqrt{\ln \frac{r}{f}};\; g(\;) = g(x) = x e^{x^2} \int_0^x e^{-x^2} du,\; u = \sqrt{\ln \frac{r_u}{r}}.$

In all practical cases the value of $r_g/r_f > 10$ so that the function $f(x)$ is the same for all tubes and is equal to $F(x) \approx .620$. For convenience in using the above formula, it can be rewritten as follows:

$$\lambda = \frac{1000\, d_p}{\sqrt{E_g}} \cdot \frac{1}{\left(\frac{d_p}{d_g}\right)} \cdot \left\{ f\left(\frac{r_g}{r_f}\right) + g\left(\frac{r_f}{r_g}\right) \right\}, \quad \begin{array}{l} for\; E_p = 0 \\ f = .620 \end{array}$$

The value of the second term is plotted on Dia.11, p.46, as a function of the ratio d_p/d_g . Knowing this ratio the value of the constant "A" can be easily determined from the curve. The use of this method makes the application of Scheibe's formula practical. The expression:

$$\frac{1000\, d_p}{\left(\frac{d_p}{d_g}\right)} \left\{ f\left(\frac{d_g}{d_f}\right) + g\left(\frac{d_p}{d_g}\right) \right\} = K_\lambda$$

can be called the "wavelength constant" of the tube, knowing which the voltage for normal waves and for higher order waves can be calculated from a simple formula:

$$\lambda_n = \frac{1}{(1+n)} \cdot \frac{K_\lambda}{\sqrt{E_g}}$$

where "n" stands for the order of the wave. For small amplitudes this formula gives the wavelength within 5%. The explaination why this formula does not hold for large amplitudes can be found in Ref.13.

A

1.5
1.4
1.3
1.2
1.1
1.0
.9
.8
.7
.6
.5
.4
.3
.2
.1

A

$$A = \frac{1}{\left(\frac{d_p}{d_g}\right)} \left\{ f\left(\frac{d_p}{d_g}\right) + g\left(\frac{d_p}{d_g}\right) \right\}_{L_p = 0}$$

$$f\left(\frac{d_p}{d_g}\right) = f\left(\sqrt{\ln \frac{r_2}{r}}\right) = f(x) = x\,e^{-x^2} \int_0^x e^{u^2}\,du \; ; \quad u = \sqrt{\ln \frac{r}{A}}$$

$$g\left(\frac{d_p}{d_g}\right) = g\left(\sqrt{\ln \frac{r_0}{r}}\right) = g(x) = x\,e^{x^2} \int_x^\infty e^{-u^2}\,du \; ; \quad u = \sqrt{\ln \frac{r_0}{r}}$$

$$\lambda_{em} = \frac{1000\,d_p}{\sqrt{E_g}} \cdot A$$

1.0 2.0 3.0 4.0 5.0 6.0 7.0 8.0 9.0 10.0 $\frac{d_p}{d_g}$

6. Energy measurements.

(a). Plate current.

It was mentioned above that the appearance of the plate current indicates the presence of oscillations in the circuit. The shape of the curves showing the plate current as a function of the tuning of the circuit resembles the shape of resonance curves (see Dia.10). Let us consider more closely in wht manner the plate current varies with the change in the A.C.potential on the plate which is superimposed on D.C. potential when oscillations are present. In an ideal case, if the cathode represented an equipotential surface, all electrons would move in straight paths radially and approach infinitely close to the plate, then the plate current could be represented by a blocked wave, as shown in Fig.12. The shaded area would represent half the number
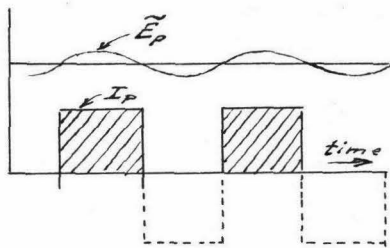
Fig. 12.

of electrons which passed the grid, and the average value ~~of the~~ of the current would be independent of the A.C. voltage. However, in the actual case, the A.C. field acts on electrons throughout the time of their motion from the filament to the plate; there exists a drop of potential along the filament and the electrons have different radial velocities due to deflections from their radial paths caused by the grid spiral. All these factors would tend to make the plate current dependent upon the magnitude of the plate potential (A.C.). As a first approximation we would expect that the plate current will be proportional to the voltage amplitude.

$$I_p \propto \widetilde{E}_{p-g}$$

This relation is confirmed by the experiment. The current in an aperiodic

Diagram 12.

I_p
m.a.

I_α
s.d.

5.0

4.5

4.0

3.5

3.0

2.5

2.0

1.5

1.0

.5

I_p

I_α

I_G

I_G

m.a.

22.5

22.0

21.5

21.0

20.5

20.0

19.5

19.0

18.5

18.0

17.5

50   100   150   200 E_g volts
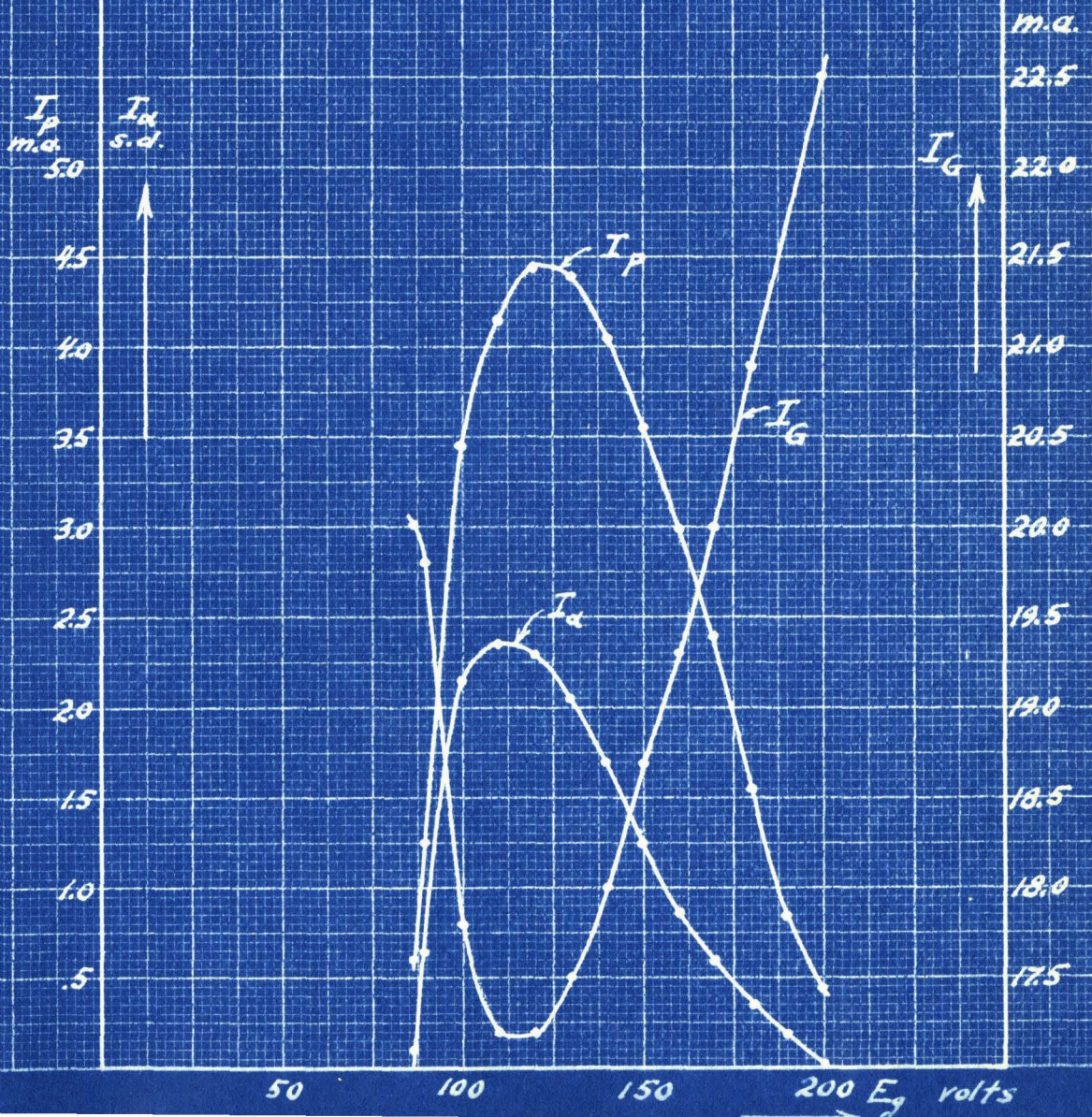
circuit coupled loosely with the Lecher system is found to be proportional to the plate current. Since the current in such an aperiodic circuit is proportional to the A.C. current in the oscillating circuit, it means then, that the plate current is proportional to the amplitude of oscillations in the circuit. The curves on Dia.12, p.48, show the plate current I_p, the grid current I_g and the current in the aperiodic circuit I_α, as
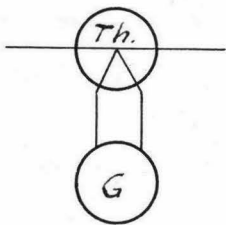
Fig. 13.

functions of the grid voltage E_g. The current in the aperiodic circuit has been measured by means of a thermocouple and a galvanometer, as shown in Fig.13. The curves on Dia.12 show that the shapes of the plate current curve and and of the current in the aperiodic circuit are alike. Thus the measurement of the plate current gives the relative value of the amplitude of oscillations. The grid current (I_g) follows the (I_α) curve more closely than does the (I_p) curve, but it is difficult to measure accurately small variations in the grid current caused by oscillations.

(b). Thermocouple method.

As was mentioned above the relative value of the intensity of oscillations can be measured by a thermocouple in the aperiodic circuit. The absolute value of the energy can not be found by this method, because the coefficient of coupling between the aperiodic circuit and the oscillating circuit, and the constant of the aperiodic circuit is difficult even to estimate, as they depend not only upon the dimensions and distances of the two circuits,

Diagram 13.

$V_E = 6.3\,v.$
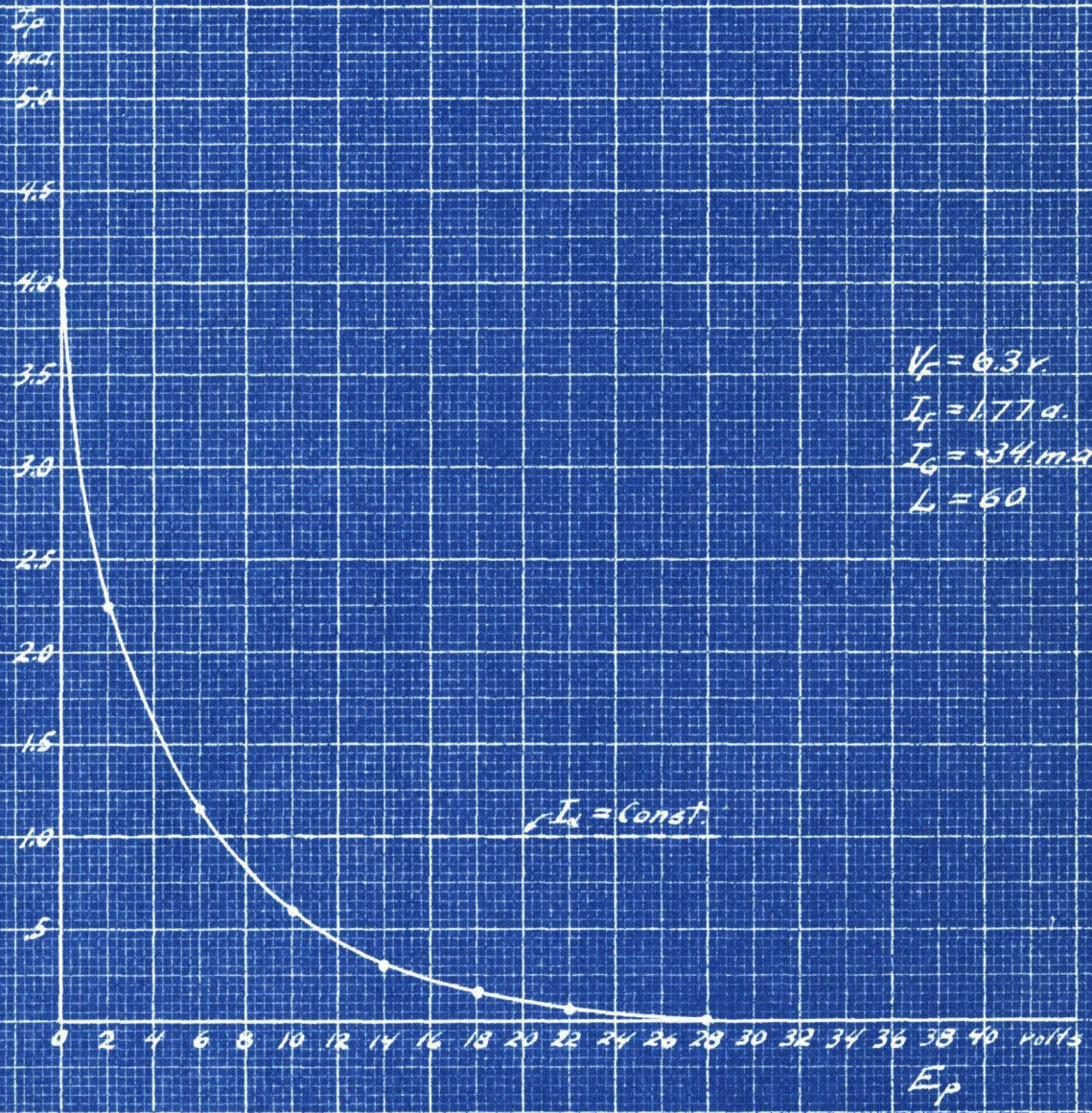$I_F = 1.77\,a.$
$I_G = -34\,m.a.$
$\angle = 60$
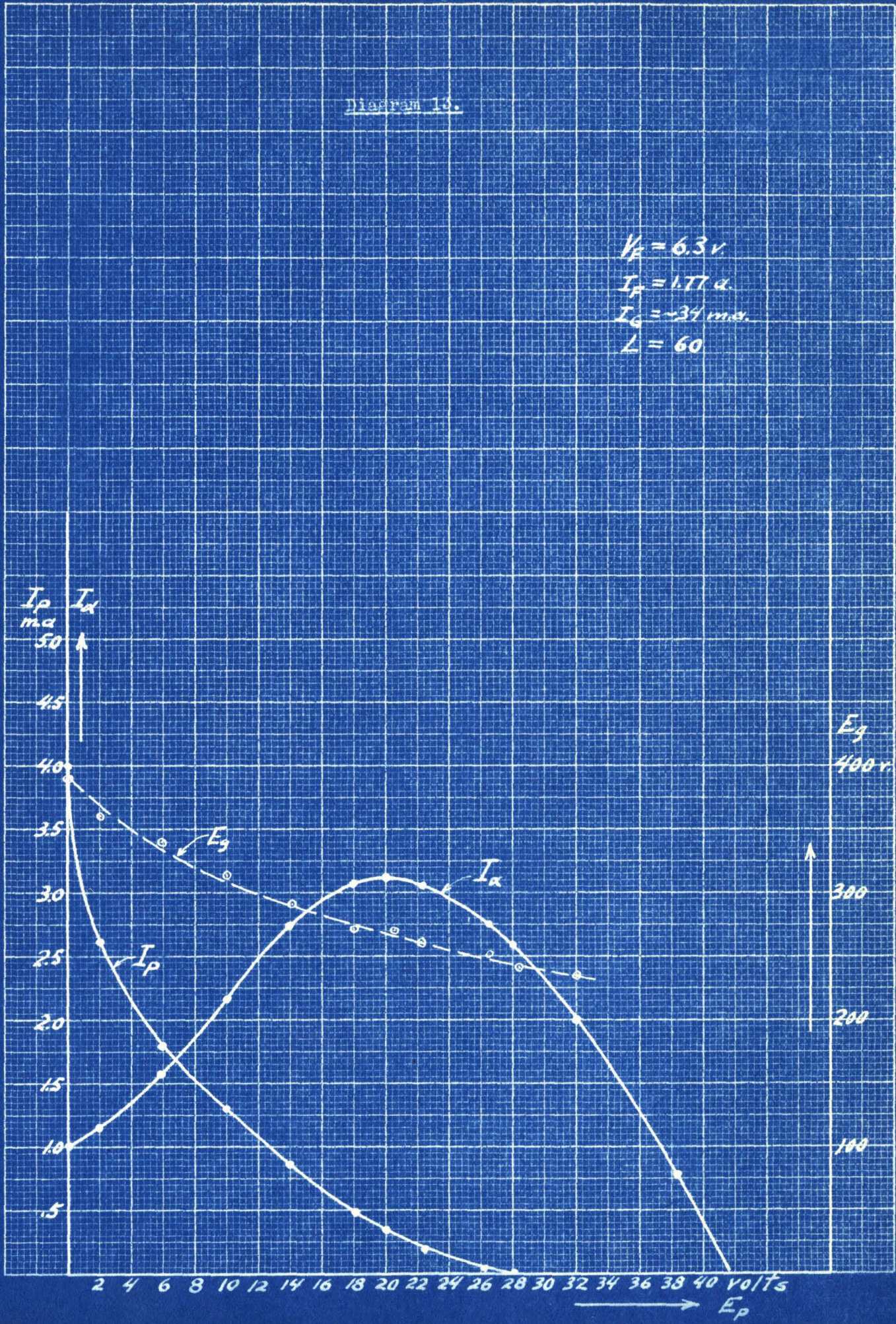
but vary also with the frequency. The thermocouple could be
placed directly in the oscillating circuit but this would
introduce a considerable resistance in the system and change
its characteristics, which is undesirable especially because
it is difficult to calculate the constants. Thus the thermo-
couple methods give only the measure of the relative change in
the intensity of oscillations.

(c). Absolute value of energy output.

Some idea of what the absolute value of the energy is, can
be obtained by the following method. It was shown that the plate
current is caused by the A.C. potential on the plate. Only those
electrons will reach the plate which acquired more than zero
energy in passing from the filament to the plate. This energy
has been taken from the A.C. energy. What becomes of this surplus
energy of the electrons which reach the plate? They strike the
plate and their energy is dissipated in the form of heat at the
plate. Thus the plate current represents loss of energy. This
was first demonstrated by Kroebel (Ref.5). Similar relults have
been obtained by the author. The curves shown on Dia.13, p.50,
were obtained when the plate potential was made negative. Here
we see that while the plate current decreases with increasing
negative plate potential, the current in the aperiodic circuit
increases. This happens because the energy which was lost at the
plate is now delivered to the oscillating circuit. The plate loss
can be measured as follows. The plate current giving the number
of electrons per second which loose their energy at the plate is
measured by the galvanometer in the plate circuit. The energy

Diagram 14.

$V_F = 6.3 \, r.$

$I_f = 1.77 \, a.$

$I_G = -34 \, ma.$

$L = 60$

$I_d = Const.$

I_p
$ma.$

5.0

4.5

4.0

3.5

3.0

2.5

2.0

1.5

1.0

.5

0 2 4 6 8 10 12 14 16 18 20 22 24 26 28 30 32 34 36 38 40 volts

E_P

distribution amongst the individual electrons must also be known to find the total plate loss. If we apply a negative potential to the plate, at the same time keeping the A.C. plate potential the same, the plate current will gradually decrease. The negative potential at which the plate current becomes zero will represent the maximum energy of the electrons. The energy distribution will be represented by a curve shown on Dia.14, p. 52; by integrating this curve the total energy loss at the plate (W_p) can be found.

The plate loss is not the only loss. Some power is expended due to resistance and radiation of the circuit. The theoretical considerations of the mechanism of oscillations of the Barkhausen tube lead one to believe that there exists an energy loss at the grid. By the grid loss here is meant not the loss $I_g E_g$, but a loss similar to the plate loss due to the oscillations. For practical purposes the radiation loss may be considered the only useful energy, so that it is desirable to eliminate all other losses as completely as possible. The ohmic resistance of the circuit is usually very small. The grid loss can be decreased by making the grid of thin wires, althogh the grid loss can not be eliminated completely. The plate loss is decreased by applying negative potential to the plate. The curves on Dia.13 show the increase of the intensity of oscillations when the plate loss is decreased. The maximum of intensity is reached when the plate current is reduced to zero. With further increase in voltage the intensity of oscillations decreases because the oscillating space charge is farther away from the plate and the voltage induced by it on the plate is smaller. The ratio I_α/I_{α_o} represents the increase

in the amplitude of oscillations which can be obtained with
optimum value of the plate voltage. If the plate loss is
measured for zero plate voltage, the maximum energy output
of the tube can be approximately calculated from the formula:

$$W_{max} \;\simeq\; W_p \left(\frac{I\alpha}{I_{\alpha_0}}\right)^2$$

## 7. Dependence of energy output upon the emission current.
a) Limits of maximum energy output.

The above derived relations are applicable to cases when the
tube is operated with constant emission current. The increase in
emission current increases the intensity of oscillations. The curves
on Diagram 15 and Dia.16 are typical curves representing the change
of the intensity of oscillations with the emission. They show that
the oscillations begin only at a certain minimum grid current. The
intensity increases very rapidly at first and then reaches saturation.
This effect is quite important since it shows that the energy output
of the Barkhausen oscillator can not be increased indefinitely by
increasing the emission. The voltage at which the saturation is reached
is approximately the voltage corresponding to the saturation current
on the static characteristic. This then, represents the upper limit
of energy which can be obtained with a given tube. This saturation
effect can be explained by the screening action of electrons which do
not deliver energy to the circuit but form a dense space charge around
the electrodes, thus disturbing the oscillations.

One interesting feature of these curves (Dia.15) is that the
minimum grid current does not depend upon the plate voltage. Another

Diagram 15.

(58)
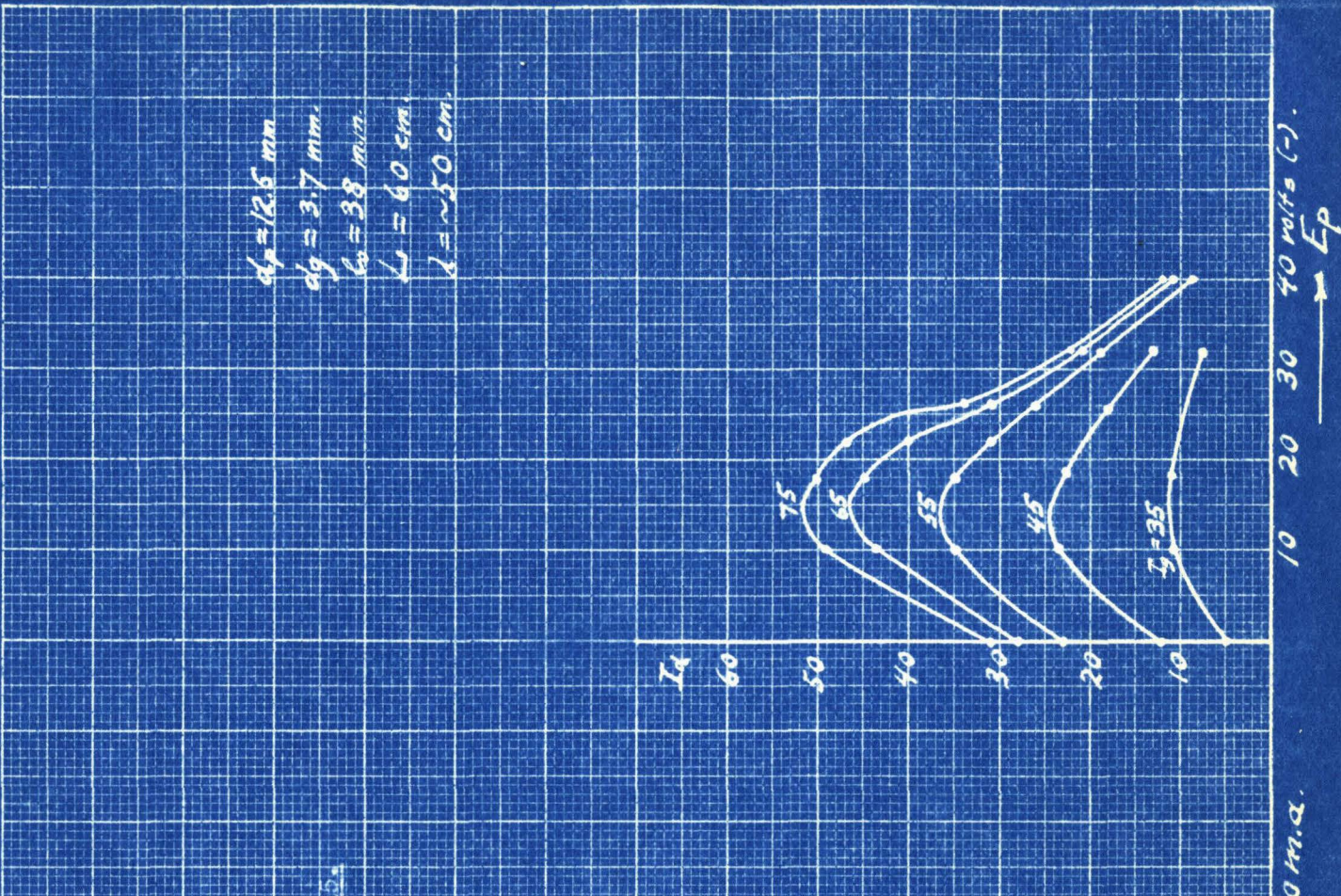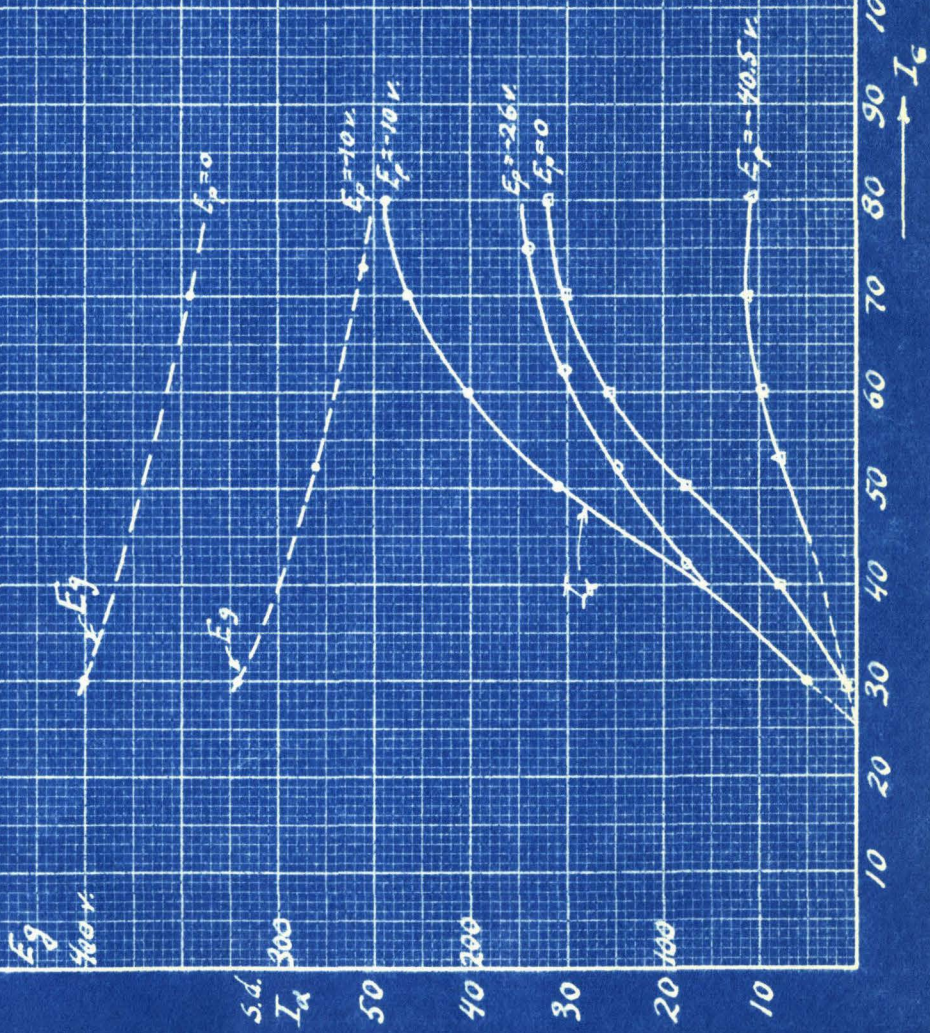
Diagram 16.
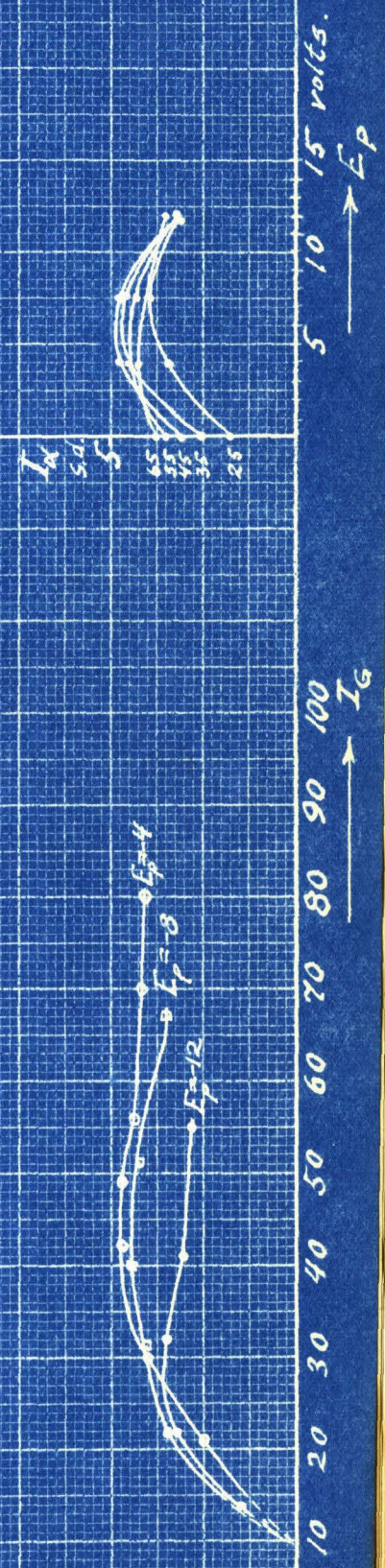
important point is that the optimum negative plate voltage is not
directly proportional to the amplitude of oscillations, but seems
to be also a function of the grid voltage and the emission current.

(b). Experience with water cooled grids.

Results similar to those shown on Dia.15, were obtained for
tubes with water cooled grids. Figures 14 and 15 show the general
view of the construction of the tubes. The saturation was also
reached at voltages corresponding to the static saturation curves.
In most cases, however, the minimum grid current was considerably
higher than for radiation cooled grids, which can be explained by
the coarseness of the grid which had to be made of tubing of larger
diameter than the diameter of wire used for radiation cooled grids.
The maximum intensity of oscillations that could be obtained with
these tubes was usually smaller than for ordinary tubes. Thus, in
general, it can be said, that the use of water cooled grids is not
a solution for increasing the energy output of the Barkhausen
oscillator, since other factors, such as symmetry, proper design
of electrodes and sharp tuning of the circuit, are of a greater
importance than the excessive heating of the grid.

(c). Minimum wavelength as a function of tube constants.

The above tests demonstrated the existance of the lower ($I_g$min)
and the upper ($I_g$max) limits of the grid current (the latter
corresponding to the maximum of energy output). Obviously, the tube
will produce oscillations only if $I_g$max$>$$I_g$min. The dependence of
$I_g$max upon the voltage can be approximately expressed as follows:
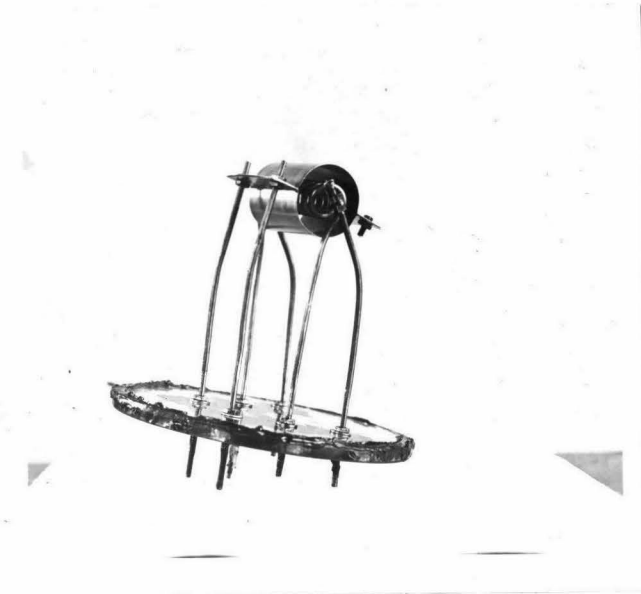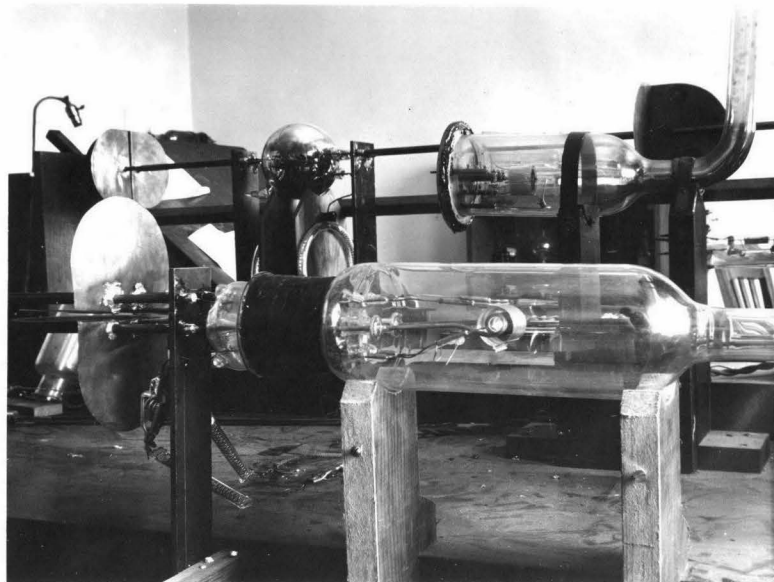
$$I_g\text{max} = k_s \, E_g^{3/2}$$

Fig. 14.

Fig. 15.

where the constant "k_s" can be called the saturation constant of the tube. It depends in a known manner upon the dimensions of the electrodes and can be calculated. In the short wave region the value of $I_g\text{min}$ can be expressed as (see p.20):

$$I_g\text{min} = \frac{k_e}{\lambda^4}$$

where "k_e" can be called the excitation constant of the tube. The condition for oscillations requires that:

$$I_g\text{min} < I_g\text{max}, \quad \text{or:} \quad \frac{k_e}{\lambda^4} < k_s \, E_g^{3/2}$$

Expressing the voltage E_g in terms of the wavelength and the wavelength constant (see p.45), we get:

$$\lambda = \frac{\kappa_\lambda}{\sqrt{E_g}} \; ; \quad E_g = \frac{\kappa_\lambda^2}{\lambda^2} \; ; \quad \therefore \; \frac{\kappa_e}{\lambda^4} < \kappa_s \frac{\kappa_\lambda^3}{\lambda^3} \quad oz \quad \lambda_{min} \geqslant \frac{\kappa_e}{\kappa_s \, \kappa_\lambda^3}$$

A similar expression for waves of order "n" will be:

$$I_{g_{min}} = \frac{\kappa_{e_n}}{\lambda_n^4} \; ; \quad I_{g_{max}} = \kappa_s E_g^{3/2} \; ; \quad \lambda_n = \frac{\kappa_\lambda}{(1+n)\sqrt{E_g}} \; ;$$

$$\therefore \quad \lambda_{n_{min.}} \geqslant \frac{\kappa_{e_n}}{\kappa_s \, \kappa_\lambda^3} \cdot \frac{1}{(1+n)^3}$$

These relations show that shorter wavelengths can be obtained for higher order waves. However, the excitation coefficient for high orders "k_{e_n}" depends a great deal upon the symmetry, so that higher order waves are obtained only when the tube is symmetrical. The value of the excitation coefficient depends not only upon the design of the tube, but also upon the nature of the oscillating circuit.

8. Conditions for maximum energy output.

The conditions for obtaining maximum energy output from the Barkhausen oscillator will be here summarized:

a) The oscillating circuit must be tuned to the most probable electronic frequency or its multiple (Ref. 1,3,4).

b) The emission current must be high, almost reaching its saturation value.

c) The plate voltage must be negative and adjusted for maximum amplitude so as to eliminate the plate loss (Ref.5).

d) The tube must be symmetrical in order that higher order waves could be obtained (Ref.7).

e) The A.C. voltage between the electrodes must be a maximum, which can be obtained by placing the electrodes in the loop of the voltage wave, as has been described in paragraph 3 of this paper.

The above are the most essential requirements. Other factors, such as the construction of the grid, the ratio of the diameters of the plate and grid, their size (diameter and length), the size and the material of the filament, the degree of vacuum in the tube, and many other factors have effect upon the operation of the tube. But a systematic study of their effects has been very difficult, since they were usually masked by the more important ones. It is hoped that this work may aid in the further study of the Barkhausen oscillator by reducing the number of the "unknowns".

In conclusion, the author wishes to express his appreciation for the assistance rendered by Mr. William Clancy in the construction of the tubes, the advice and suggestions by Dr. S.S.Mackeown, and the interest in this work shown by Professor R.W.Sorensen and Dr. R.A.Millikan.

References:

1. H.Barkhausen and K.Kurz, Phys.ZS, 21, 1, 1920.

2. H.E.Hollmann, ZS für Hochfrequenztechnik, 33, 1929, pp.27,66,101.

3. G.Potapenko, ZS f.T.Phys., 1929, p.542.

4. G.Potapenko, Phys.Rev., Vol.39, 4, 1932, p.625, 638.

5. W.Kroebel, ZS f. Phys.,61, 3,4.

6. E.Gill and J.Morrell, Phil.Mag., 44, 161, 1922.

7. A.Wainberg, Journal of Applied Physics, Vol.VII, I, 1930. (Russ.).

8. N.Kapzov, ZS f. Phys., 129, 1925.

9. F.Ollendorff, Die Grundlagen der Hochfrequenztechnik, Berlin, 1926.

10. H.G.Müller, Elektrische Nachrichtentechnik, April 5, 1930.

11. H.E.Hollmann, Ann. d. Phys., 86, 1928, p.1062.

12. A.Scheibe, Ann.d.Phys., 73, 54, 1925.
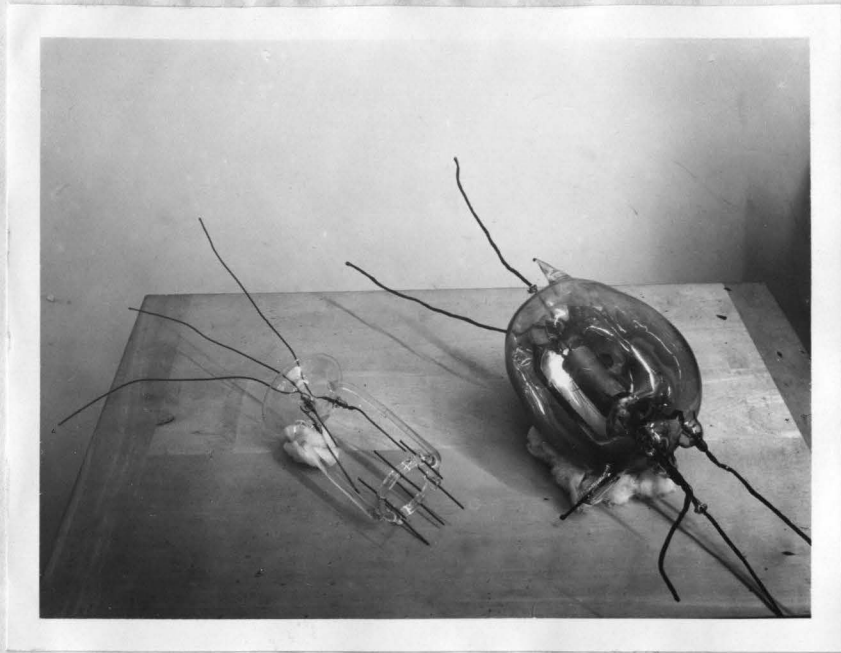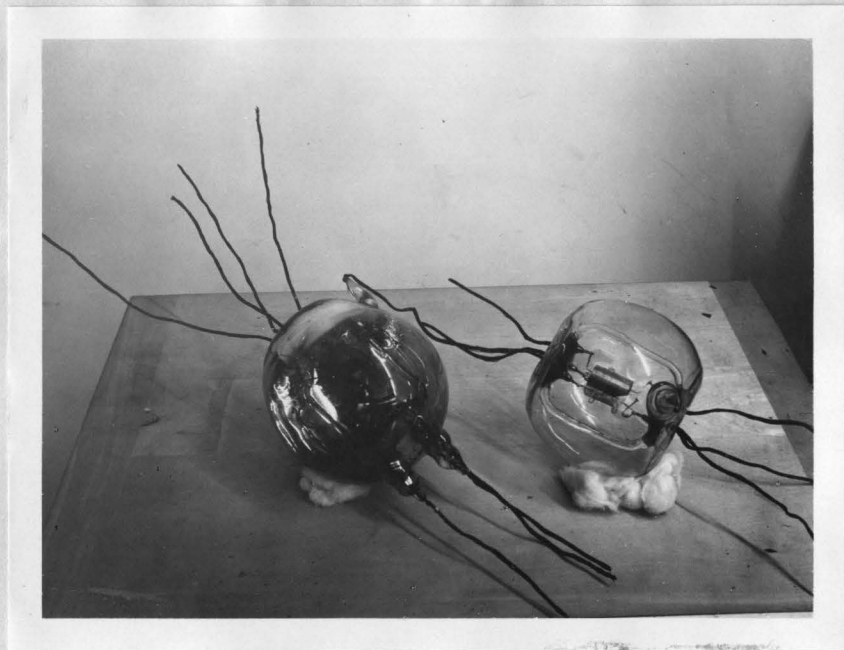
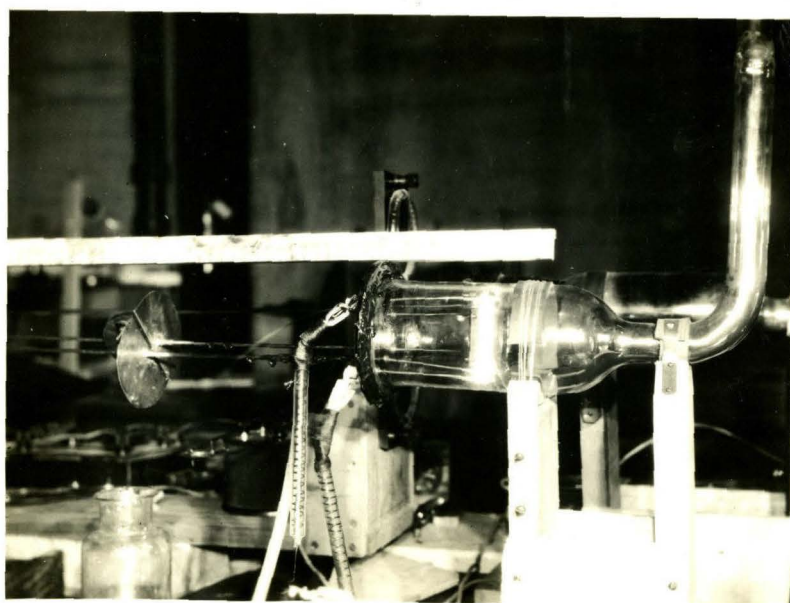13. G.Potapenko, Phys.Rev., Vol.39, 3, p. 547, (Abstract).
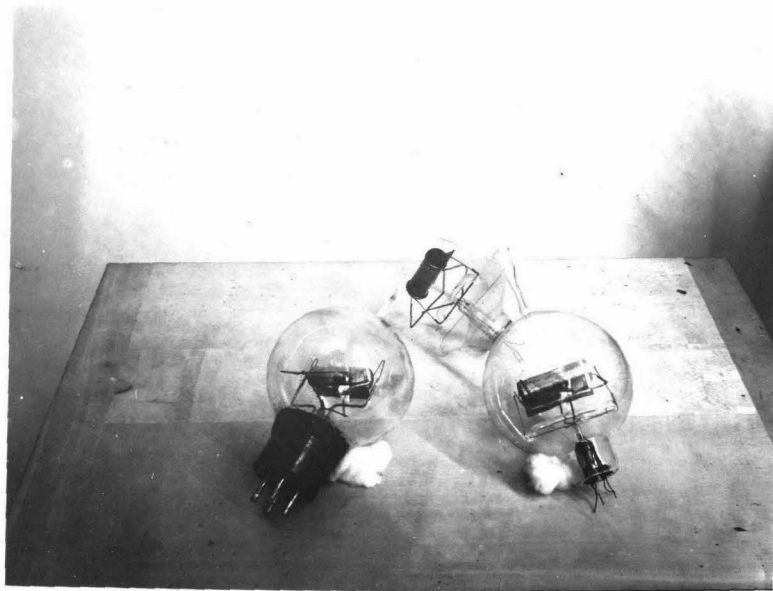
Fig. 16.
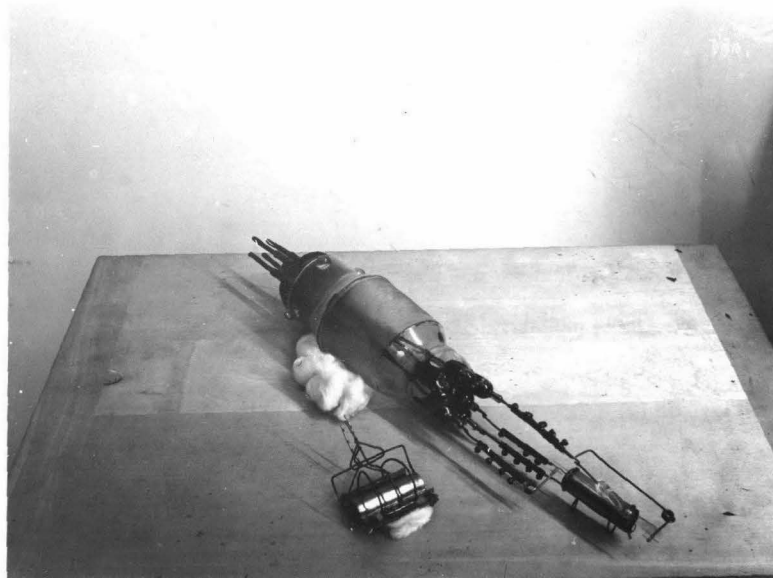
Fig. 17.

Fig. 18

Fig. 19.

Fig. 20

Fig. 21.